
TabUnite: An Efficient Encoding Framework for Tabular Data Generation

Anonymous Author(s)

Affiliation

Address

email

Abstract

1 Generative models for tabular data face a long-standing challenge in the effective
2 modelling of heterogeneous feature interrelationships, especially for generating
3 tabular data with both continuous and categorical input features. Capturing these
4 interrelationships is crucial as it allows models to understand complex patterns
5 and dependencies that exist in the underlying data. A promising option to ad-
6 dress the challenge is to devise suitable encoding/embedding schemes for the
7 input features before the generative modelling process. However, prior methods
8 often rely on either suboptimal heuristics such as one-hot encoding of discrete
9 features and separated modelling of discrete/continuous features, or latent space
10 generative models. Instead, our proposed solution leverages efficient continuous
11 encodings to unify the data space and applies a single generative process across
12 all the encodings jointly, thereby efficiently capturing heterogeneous feature inter-
13 relationships. Specifically, it employs encoding schemes such as Analog Bits or
14 Dictionary Encoding that effectively convert discrete features into continuous ones.
15 Extensive experiments on real-world and synthetic tabular datasets comprising of
16 heterogeneous features demonstrate that our encoding schemes, combined with
17 Flow Matching as the generative model, significantly enhances model capabilities.
18 Our models, TabUnite-i2bFlow and TabUnite-dicFlow, are able to address data
19 heterogeneity, achieving superior performances across a broad suite of datasets,
20 baselines, and benchmarks while generating accurate, robust, and diverse tabular
21 data.

22 1 Introduction

23 Tabular data is omnipresent in data ecosystems of many sectors such as healthcare, finance, and
24 insurance (Clare et al., 2014; Moro et al., 2012; Datta, 2020). These industries utilise tabular data
25 generation for many practical purposes, including imputing missing values, reducing sparse data,
26 and better handling imbalanced datasets (Jolicoeur-Martineau et al., 2024; Onishi & Meguro, 2023;
27 Sauber-Cole & Khoshgoftaar, 2022). However, generative models face challenges inherent to tabular
28 data including feature heterogeneity (Liu et al., 2023). Unlike homogeneous data modalities such
29 as images or text, tabular data often contain mixed feature types, ranging from (dense) continuous
30 features to (sparse) categorical features. More importantly, these tabular features, regardless of
31 form, are intertwined contextually (Borisov et al., 2023). For example, the numerical salary of a
32 person is correlated to their categorical age and education (Becker & Kohavi, 1996). Therefore
33 capturing the interrelationships between tabular heterogeneous features is crucial, as it allows models
34 to incorporate contextual knowledge for understanding complex patterns and dependencies in the
35 underlying data. Additionally, an increasing demand is observed for larger tabular generative models
36 trained potentially on many different datasets, where the capability to model heterogeneous feature
37 spaces across datasets is of utmost importance (van Breugel & van der Schaar, 2024).

38 A promising solution for the feature heterogeneity challenge is to devise suitable encoding/embedding
39 schemes for pre-processing the input features before applying the generative model. However, existing
40 methodologies often rely on (1) separate generative processes on discrete & continuous features
41 which do not model their correlations properly, (2) sub-optimal encoding heuristics, or (3) learned
42 latent embedding which is parameter inefficient. For example, the one-hot encoding approach for
43 categorical variables leads to sparse representations in high dimensions, where generative models are
44 susceptible to under-fitting (Krishnan et al., 2017; Poslavskaya & Korolev, 2023). On the other hand,
45 creating a latent embedding space requires training an additional embedding model based on e.g.,
46 ResNet (He et al., 2015) or a Transformer-based β -VAE (Higgins et al., 2017; Kingma & Welling,
47 2013; Zhang et al., 2023) and trained using e.g., self-supervised learning (Chen et al., 2020). Hence,
48 the quality of latent space generative models also depends on the embedding model’s capability to
49 capture the underlying dependency structure of the tabular data. Overall, proper pre-processing of
50 heterogeneous features is crucial for high-quality tabular data generation, and poor encoding schemes
51 for the data features can lead to information loss that can not be recovered from the generative model.

52 The goal of our work is to generate high-quality synthetic tabular data by employing (1) *proficient*
53 *categorical encoding schemes* to unify the data space. This enables a single generative model to be
54 applied while enforcing a (2) *fast and efficient sampling* procedure. In summary, our contributions
55 are as follows:

- 56 1. We devise two categorical encoding schemes using Analog Bits (Chen et al., 2022) and
57 Dictionary Encoding (partially inspired by Mairal et al. (2008, 2009)) that seamlessly
58 convert categorical variables into an efficient and compact continuous representation. By
59 facilitating the model to generate data in a unified continuous space, we can “unite” the mixed
60 features to capture heterogeneous feature interrelationships based on a single generative
61 model on continuous inputs. Empirically, under our encoding schemes, the model learns to
62 accommodate the heterogeneity of tabular features.
- 63 2. We employ Flow Matching (Lipman et al., 2022; Liu et al., 2022; Tong et al., 2023) as our
64 generative model. It is a simulation-free framework for training continuous normalizing flow
65 models (Chen et al., 2019) by replacing the stochastic diffusion process with a predefined
66 probability path constructed with theories from optimal transport (McCann, 1997). Our
67 results showcase that combining our categorical encoding schemes with Flow Matching
68 speeds up the sampling speed dramatically, saving time and computation power, while
69 enhancing the generation quality. Consequently, we propose two models: TabUnite-i2bFlow
70 and TabUnite-dicFlow. Both models achieve superior performances across a wide spectrum
71 of tabular data generation baselines, datasets, and benchmarks. The architecture of our
72 models is illustrated in Figure 1.
- 73 3. We curate a large-scale heterogeneous tabular dataset from the Census dataset (Meek et al.,
74 2001) with over 80 features of mix-types and over 2.4 million samples. This new benchmark
75 is significantly more challenging for tabular generative models than existing benchmarks
76 from public data repositories (Dua & Graff, 2017; Vanschoren et al., 2013) which often
77 have $< 100k$ datapoints and ≤ 30 features. It reflects better on the scalability of tabular
78 generative models, where our empirical results again reveal the importance of good encoding
79 schemes for heterogeneous features.

80 2 Related Works

81 **Generative Models in Tabular Data Generation.** The latest tabular data generation methods have
82 made considerable progress compared to traditional methods such as Bayesian networks (Rabaey
83 et al., 2024) and SMOTE (Chawla et al., 2002). CTGAN and TVAE (Xu et al., 2019) were two
84 models based on the Generative Adversarial Network (Goodfellow et al., 2014) and Variational
85 Autoencoder (Kingma & Welling, 2013) architectures respectively. These models were applied along
86 with techniques such as conditional generation and mode-specific normalization to further learn
87 column-wise correlation. Other works such as GReaT (Borisov et al., 2023) and GOGGLE (Liu
88 et al., 2023) saw successes with the use of graph neural networks and autoregressive transformer
89 architectures respectively in performing tabular data synthesis. Recently, Diffusion (Ho et al., 2020)
90 and Flow Matching (Lipman et al., 2022) provided new avenues for exploration within the tabular
91 domain. This included STaSy (Kim et al., 2022), which employed a score-matching diffusion model

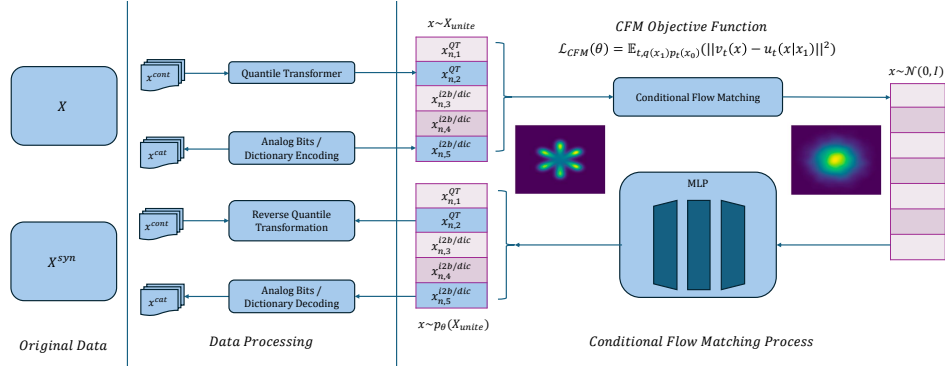


Figure 1: TabUnite-i2bFlow and TabUnite-dicFlow Architecture. Continuous features x^{cont} are encoded via a QuantileTransformer (Pedregosa et al., 2011). Categorical data x^{cat} are encoded using Analog Bits or Dictionary Encoding methods. With an efficient continuous data space, we apply Conditional Flow Matching as our generative model where we ultimately synthesise samples. These samples are then mapped back to their original representation via their respective decoding schemes.

92 paired with techniques such as self-paced learning and fine-tuning to stabilise the training process,
 93 and CoDi (Lee et al., 2023), which utilised separate diffusion schemes for categorical and numerical
 94 data along with interconditioning and contrastive learning to improve the synergy among different
 95 features. TabDDPM (Kotelnikov et al., 2023) presented a similar diffusion scheme compared to
 96 CoDi and showed that the simple concatenation of categorical and numerical data before and after
 97 denoising led to improvements in performance. The most recent work in this domain was TabSYN
 98 (Zhang et al., 2023), a latent diffusion model which transformed features into a unified embedding
 99 via a feature tokenizer before applying EDM diffusion (Karras et al., 2022) to generate synthetic data.

100 **Encoding Schemes.** CoDi (Lee et al., 2023) and TabDDPM (Kotelnikov et al., 2023) utilised a
 101 separated data space, where Gaussian Diffusion (Ho et al., 2020) was performed on numerical
 102 columns and Multinomial Diffusion (Hoogeboom et al., 2021) was performed on categorical columns,
 103 with some additional techniques used to bind the two separate diffusion models. However, learning
 104 the cross-correlation among various features through separate methods was often less effective than
 105 conducting diffusion directly across a unified data space that included all features in the dataset. To
 106 achieve this, various encoding schemes were employed to process both categorical and numerical
 107 data so they occupy the same data space. One of the most widely used methods was one-hot encoding,
 108 which was used in both STaSy (Kim et al., 2022) and TabSYN (Zhang et al., 2023) that encoded
 109 categorical columns. One-hot encoding transformed categorical variables into a binary vector, where
 110 each category was populated with 0's with the exception of a single 1 that indicated the presence
 111 of a particular category. On top of one-hot encoding, TabSYN (Zhang et al., 2023) further used
 112 a column-wise feature tokenization technique that together transformed numerical and categorical
 113 features all into shared embeddings of the same length.

114 **Flow Methods.** Flow methods were introduced to the field of diffusion-based deep generative
 115 models as Probability Flow ODEs (Song et al., 2021), which, originally based on the concept of
 116 normalizing flows (Rezende & Mohamed, 2016), allowed for deterministic inference and exact
 117 likelihood evaluation. Compared to other diffusion-based methods such as score-matching (Song
 118 et al., 2021), DDPM (Ho et al., 2020), and DDIM (Song et al., 2022), flow-based models used
 119 continuous transformations defined by neural ODEs, to map samples from a simple distribution to
 120 samples from a more complex target distribution. This allowed for efficient density estimation and
 121 generation of high-dimensional data. In the context of tabular data, Flow Matching was applied to
 122 gradient-boosted trees in place of neural networks to learn the vector field (Jolicœur-Martineau et al.,
 123 2024).

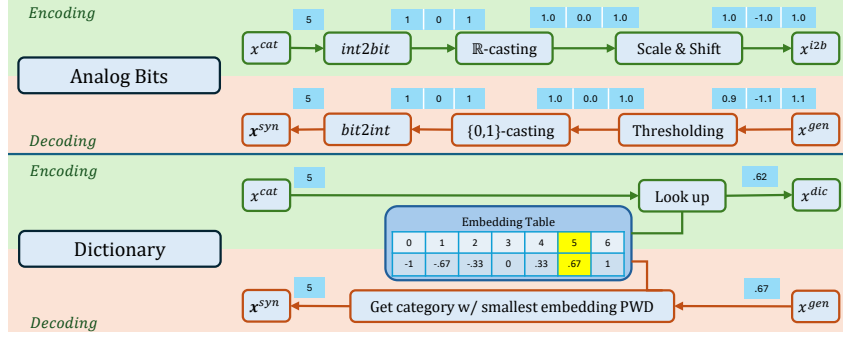


Figure 2: TabUnite Encoding Methods. We leverage Analog Bits & Dictionary encoding to transform categorical features into a compact and efficient continuous representation before applying a single unified generative model to synthesise tabular data.

124 3 TabUnite Models

125 Before diving into our methodology, we begin the section with preambles regarding a high-level
 126 overview of the tabular setting. Here a tabular dataset is characterized as $\mathbf{X} = \{\mathbf{x}_i\}_{i=1}^N$ with N
 127 samples (rows), where a datapoint $\mathbf{x}_i \in \mathbb{R}^{D_{\text{cont}}} \times \mathbb{N}^{D_{\text{cat}}}$ comprises of D_{cont} continuous features and
 128 D_{cat} categorical features. We denote each \mathbf{x}_i as $\mathbf{x}_i := [x_{i,1}^{\text{cont}}, \dots, x_{i,D_{\text{cont}}}^{\text{cont}}, \dots, x_{i,1}^{\text{cat}}, \dots, x_{i,D_{\text{cat}}}^{\text{cat}}]$.

129 Our goal is to generate synthetic data samples, \mathbf{x}^{syn} , that mimic the quality of the real data, \mathbf{X} . To do
 130 so, we are required to learn a parameterized generative model known as $p_{\theta}(\mathbf{X})$, from which \mathbf{x}^{syn} can
 131 be sampled. Prior to learning, extensive data pre-processing is required where categorical features
 132 are encoded into continuous features: $f(x^{\text{cat}}) = x^{\text{enc}}$, where f denotes the encoder. Poor or sparse
 133 feature encoding of categorical features can hinder the model’s ability to learn effectively. Therefore,
 134 we devise efficient and effective encoding schemes to address this issue.

135 3.1 Encoding Schemes

136 We explore Analog Bits (Chen et al., 2022) and Dictionary to encode categorical features. note that
 137 continuous features are encoded using the QuantileTransformer (Pedregosa et al., 2011) where we
 138 follow TabSYN’s and TabDDPM’s methodology (Zhang et al., 2023; Kotelnikov et al., 2023).

139 **Analog Bits Encoding.** A categorical feature that has K unique categories, $x^{\text{cat}} \in \{0, \dots, K-1\}$,
 140 can be expressed using $\lceil \log_2(K) \rceil$ binary bits. For example, a categorical feature with $K = 5$
 141 categories is expressed using $\lceil \log_2(5) \rceil = 3$ bits with an embedding function $f(x^{\text{cat}}) = x^{\text{enc}} \equiv x^{i2b}$
 142 that maps $x^{\text{cat}} \in \{0, 1, 2, 3, 4\}$ to $x^{i2b} \in \{000, 001, 010, 100, 101\}$ respectively. Subsequently,
 143 each binary bit is cast into a real-valued representation, followed by a shift and scale formula:
 144 $x^{i2b} = (x^{i2b} \cdot 2 - 1)$. This transformation shifts and scales the binary values $\{0, 1\}$ to $\{-1, 1\}$.
 145 Thus, training and sampling of continuous-feature generative models (e.g., diffusion models) become
 146 computationally tractable. For generations, thresholding and rounding are applied to the generated
 147 continuous bits from the model to convert them back into binary form, which can be decoded trivially
 148 back into the original categorical values.

149 **Dictionary Encoding.** A categorical feature that has K unique categories, $x^{\text{cat}} \in \{0, \dots, K-1\}$,
 150 can be expressed using a look-up embedding table function which encodes the categories to equally
 151 spaced real-valued representations within the range $[-1, 1]$. Note that when a categorical feature
 152 contains more categories, the embedding requires a larger range to prevent the values from being
 153 too close to each other, hindering the model’s ability to distinguish between categories. This can
 154 be addressed by increasing the range accordingly. The encoding function is defined as follows:
 155 $f(x^{\text{cat}}) = x^{\text{enc}} \equiv x^{\text{dic}} = -1 + \frac{2x^{\text{cat}}}{K-1}$. For example, a categorical feature with $K = 5$ categories
 156 is encoded using the look-up table function, $f(x^{\text{cat}})$, that maps $x^{\text{cat}} \in \{0, 1, 2, 3, 4\}$ to $x^{\text{dic}} \in$
 157 $\{-1, -0.5, 0, 0.5, 1\}$ respectively. Consequently, this also ensures the preservation of the intrinsic
 158 order in ordinal data. To perform decoding, the Euclidean pairwise distance between x^{gen} and each
 159 of the K categorical embeddings is calculated. The categorical value that corresponds to the nearest
 160 embedding vector is chosen. In our experiments, we use a 1-dimensional encoding setup described

161 above. We can also extend Dictionary Encoding to n dimensions when there is a need to capture
 162 more nuanced patterns in complex datasets. We create an embedding matrix $M \in \mathbb{R}^{K,n}$ by filling
 163 it with randomly sampled values from a standard normal distribution $\mathcal{N}(0, 1)$. We then normalise
 164 this embedding matrix by scaling the values of each column linearly to the range $[-1, 1]$, using each
 165 column’s minimum and maximum values. The resulting matrix is our Dictionary, where we denote
 166 the lookup operation as function f .

167 In Figure 2, we consider an example categorical data point of $x^{cat} = 5$ with $K = 7$ categories
 168 where $x^{cat} \in \{0, 1, 2, 3, 4, 5, 6\}$. Analog Bits can encode $x^{cat} = 5$ into $\lceil \log_2(7) \rceil = 3$ bits where we
 169 deemed it to be $x^{i2b} = 101$. It is then cast into \mathbb{R} followed by the scale and shift formula. Dictionary
 170 creates a look-up embedding table where the different categories are distributed evenly as a real
 171 number within the range $[-1, 1]$. In our example, $x^{cat} = 5$ is mapped to $x^{dic} = .67$ by the table. A
 172 similar reverse process is applied to both methods for obtaining the decoded representations.

173 In contrast to traditional one-hot categorical encoding, our encoding methods offer more efficient and
 174 dense representations. One-hot encoding can lead to high-dimensional sparse vectors (Poslavskaya &
 175 Korolev, 2023) and cause underfitting when learning from it (Krishnan et al., 2017). On the contrary,
 176 Analog Bits encoding reduces dimensionality whereas Dictionary encoding transforms the data into a
 177 more compact format, preserving the intrinsic relationships between categories. This efficiency can
 178 lead to faster training/sampling times, and improved performance in machine learning models by
 179 leveraging continuous representations for categorical data. Comparing our two encoding methods,
 180 Dictionary encoding is preferred when converting *ordinal* categorical data due to the presence of an
 181 intrinsic ordering among the categories that are preserved in the embedding space.

182 3.2 Conditional Flow Matching

183 After encoding our continuous and categorical columns, we are presented with a unified and continu-
 184 ous data space, $\mathbf{X}_{i2b} \in \mathbb{R}^{N \times (D_{cont} + \lceil \log_2(D_{cat}) \rceil)}$ and $\mathbf{X}_{dic} \in \mathbb{R}^{N \times (D_{cont} + D_{cat} \times n)}$. For convenience,
 185 we define \mathbf{X}_{unite} to represent either \mathbf{X}_{i2b} or \mathbf{X}_{dic} , depending on the encoding method used. Sub-
 186 sequently, we apply Conditional Flow Matching (Lipman et al., 2022) as our generative model
 187 to synthesise our tabular data. The Flow matching models built on top of the feature encodings
 188 with Analog Bits (“i2b”) and Dictionary (“dic”) encodings are referred to as TabUnite-i2bFlow and
 189 TabUnite-dicFlow, respectively.

190 Let \mathbf{x} denote a sample from the dataset \mathbf{X}_{unite} , i.e. $\mathbf{x} \sim \mathbf{X}_{unite}$. We learn a vector field $v_t(\mathbf{x})$ to
 191 approximate the true vector field $u_t(\mathbf{x}|\mathbf{x}_1)$, yielding an objective function of the following:

$$L_{CFM}(\theta) = \mathbb{E}_{q(\mathbf{x}_1), p_t(\mathbf{x}|\mathbf{x}_1)} \|v_t(\mathbf{x}) - u_t(\mathbf{x}|\mathbf{x}_1)\|^2 \quad (1)$$

192 This in turn generates a probability density path $p_t(\mathbf{x}|\mathbf{x}_1)$. In order to generate the path $p_t(\mathbf{x}|\mathbf{x}_1)$ via
 193 vector field $u_t(\mathbf{x}|\mathbf{x}_1)$, we consider the flow ψ_t :

$$[\psi_t]_* p(\mathbf{x}) = p_t(\mathbf{x}|\mathbf{x}_1) \quad (2)$$

194 where $\psi_t(\mathbf{x}) = \sigma(\mathbf{x}_1)\mathbf{x} + \mu_t(\mathbf{x}_1)$. This property helps establish a probability path from the noise
 195 distribution $p_0(\mathbf{x}|\mathbf{x}_1) = p(\mathbf{x})$ to $p_t(\mathbf{x}|\mathbf{x}_1)$. With the simple affine map property of ψ_t , we use it to
 196 solve for vector field u :

$$u_t(\mathbf{x}|\mathbf{x}_1) = \frac{\sigma'_t(\mathbf{x}_1)}{\sigma_t(\mathbf{x}_1)}(\mathbf{x} - \mu_t(\mathbf{x}_1)) + \mu'_t(\mathbf{x}_1) \quad (3)$$

197 generating Gaussian probability path $p_t(\mathbf{x}|\mathbf{x}_1)$. Lastly, by integrating optimal transport theories, the
 198 final objective function is the following:

$$L_{CFM}(\theta) = \mathbb{E}_{t, q(\mathbf{x}_1), p(\mathbf{x}_0)} \|v_t(\psi_t(\mathbf{x}_0)) - (\mathbf{x}_1 - (1 - \sigma_{min})\mathbf{x}_0)\|^2 \quad (4)$$

199 Relative to other generative models, particularly Diffusion, Conditional Flow Matching synthesises
 200 tabular data with a much higher sampling speed while also attaining a better generalization.

201 4 Experiments

202 We evaluate the performance of TabUnite-i2bFlow (Analog Bits + Flow Matching) and TabUnite-
 203 dicFlow (Dictionary encoding + Flow Matching) on a wide range of real-world and synthetic datasets,
 204 benchmarks, and compare the proposed models with a comprehensive number of baselines.

Table 1: AUC (classification) and RMSE (regression) scores of Machine Learning Efficiency. \uparrow indicates that the higher the score, the better the performance, vice versa. Values bolded in **red** and **blue** are the best and second best-performing models respectively. Details are found in Appendix C.

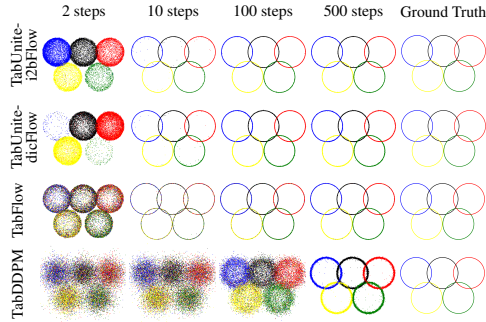
Methods	Adult	Default	Shoppers	Magic	Beijing	News	Overall Rank
	AUC \uparrow	AUC \uparrow	AUC \uparrow	AUC \uparrow	RMSE \downarrow	RMSE \downarrow	
Real	0.927 \pm 0.000	0.770 \pm 0.005	0.926 \pm 0.001	0.946 \pm 0.001	0.423 \pm 0.003	0.842 \pm 0.002	N/A
SMOTE	0.899 \pm 0.007	0.741 \pm 0.009	0.911 \pm 0.012	0.934 \pm 0.008	0.593 \pm 0.011	0.897 \pm 0.036	5
CTGAN	0.886 \pm 0.002	0.696 \pm 0.005	0.875 \pm 0.009	0.855 \pm 0.006	0.902 \pm 0.019	0.880 \pm 0.016	8
TVAE	0.878 \pm 0.004	0.724 \pm 0.005	0.871 \pm 0.006	0.887 \pm 0.003	0.770 \pm 0.011	1.01 \pm 0.016	8
GOGGLE	0.778 \pm 0.012	0.584 \pm 0.005	0.658 \pm 0.052	0.654 \pm 0.024	1.09 \pm 0.025	0.877 \pm 0.002	11
GReaT	0.844 \pm 0.005	0.755 \pm 0.006	0.902 \pm 0.005	0.888 \pm 0.008	0.653 \pm 0.013	OOM	7
STaSy	0.906 \pm 0.001	0.752 \pm 0.006	0.914 \pm 0.005	0.934 \pm 0.003	0.656 \pm 0.014	0.871 \pm 0.002	4
CoDi	0.871 \pm 0.006	0.525 \pm 0.006	0.865 \pm 0.006	0.932 \pm 0.003	0.818 \pm 0.021	1.21 \pm 0.005	10
TabDDPM	0.910\pm0.001	0.761\pm0.004	0.915\pm0.004	0.932 \pm 0.003	1.91 \pm 0.680	3.46 \pm 1.25	6
TabSYN	0.906 \pm 0.001	0.755 \pm 0.004	0.918\pm0.004	0.935 \pm 0.003	0.586 \pm 0.013	0.862 \pm 0.021	3
TabUnite-i2bFlow	0.911\pm0.001	0.763\pm0.004	0.918\pm0.005	0.941\pm0.003	0.543\pm0.007	0.847\pm0.014	1
TabUnite-dicFlow	0.911\pm0.002	0.758 \pm 0.006	0.908 \pm 0.006	0.943\pm0.003	0.555\pm0.006	0.848\pm0.013	2

205 **Datasets.** The datasets in our experiments are from the UCI Machine Learning Repository (Dua &
206 Graff, 2017), synthetic toy datasets (Chen et al., 2018), and our own self-curated dataset, ‘‘Census
207 Synthetic’’. The real-world UCI tabular datasets are chosen because they were previously utilised
208 to evaluate the existing baselines. Next, we leverage synthetic toy datasets to prove the faithfulness
209 of our model. Lastly, we curate a dataset that is much larger than existing datasets in the number
210 of samples (approx. 2.5 million samples) and comes with a large set of mixed features (approx. 40
211 and 41 categorical and continuous features each). The training/validation/testing sets are split into
212 80/10/10% apart from the Adult dataset which we adhere to its original documented splits. Full
213 details of the datasets can be found in Appendix C.1.

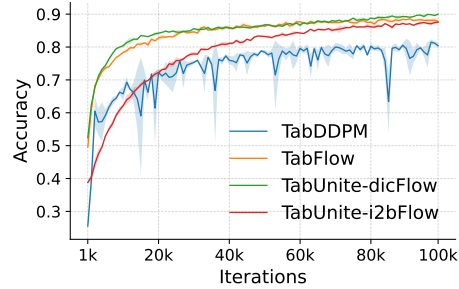
214 **Baselines: Existing modeling approaches.** We compare our model against eight other existing
215 methods for tabular generation. This includes CTGAN (Xu et al., 2019), TVAE (Xu et al., 2019),
216 GOGGLE (Liu et al., 2023), GReaT (Borisov et al., 2023), TabDDPM (Kotelnikov et al., 2023),
217 STaSy (Kim et al., 2022), CoDi (Lee et al., 2023), and, TabSYN (Zhang et al., 2023). SMOTE
218 (Chawla et al., 2002), an interpolation-based method, is also included as a base reference model. The
219 results from CTGAN, TVAE, GOGGLE, GReaT, STaSy, and CoDi are taken from the TabSYN paper
220 (Zhang et al., 2023). The main competitors to our model are TabSYN and TabDDPM since they are
221 the best-performing models to date. Hence, we reproduce the results of TabSYN and TabDDPM per
222 the recommended hyperparameters mentioned by the authors of their respective papers. More details
223 regarding these baselines can be found in Appendix C.2.

224 **Ablations: Encoding schemes and generative models (Flow/Diffusion).** We conduct our ablation
225 studies with respect to various encoding schemes and generative models. This assists us in proving
226 the effectiveness of our encoding schemes (Analog Bits and Dictionary) as well as Flow Matching
227 (Lipman et al., 2022) as the generative model. The detailed implementations of these ablations are
228 introduced in Appendix C.3.

229 **Benchmarks & metrics.** We evaluate the generative performance on a broad suite of benchmarks
230 from TabSYN (Zhang et al., 2023). We analyse the capabilities in *downstream tasks* such as machine
231 learning efficiency, where we determine the AUC score for classification tasks and RMSE for
232 regression tasks of a tabular data classifier (XGBoost (Chen & Guestrin, 2016)) on the generated
233 synthetic datasets. Next, we conduct experiments on *low-order statistics* where we perform column-
234 wise density estimation (CDE) and pair-wise column correlation (PCC). Lastly, we examine the
235 models’ quality on *high-order metrics* such as α -precision and β -recall scores (Alaa et al., 2022).
236 We add two extra benchmarks (part of Appendix C.4) including a detection test metric, Classifier
237 Two Sample Tests (C2ST) (SDMetrics, 2024) and a privacy preservation metric, Distance to Closest
238 Record (DCR) (Minieri, 2022). Further details regarding this section can be found in Appendix C.4.



(a) Qualitative Synthetic Toy Dataset.



(b) Quantitative Synthetic Toy Dataset.

Figure 3: (a) The x -axis illustrates the sampling steps and the “Ground Truth” of the dataset whereas the y -axis depicts the methods. TabUnite methods are faithful in generating high-quality samples that match the ground truth in a short period of sampling duration. (b) The x -axis illustrates the training iterations whereas the y -axis depicts the accuracy of the generated categorical columns. Training TabUnite methods are stable and converge at a higher accuracy when compared to TabDDPM.

239 4.1 Model Comparisons on Predefined Baselines

240 We benchmark TabUnite-i2bFlow and TabUnite-dicFlow across 6 datasets, against a wide range
 241 of baselines, in terms of a downstream task (machine learning efficiency) – XGBoost’s clas-
 242 sification/regression performance (Chen & Guestrin, 2016) trained on generated synthetic data
 243 (AUC/RMSE). Following the setting in TabDDPM and TabSYN (Kotelnikov et al., 2023; Zhang
 244 et al., 2023), we split the datasets into training and testing sets where the generative models are
 245 trained on the training set. Synthetic samples of equivalent size are then generated based on the
 246 trained generative models. The generated data is subsequently evaluated against the mentioned
 247 benchmarks, using the testing set—unseen during training and generation phases—to assess the
 248 models’ performance and generalization.

249 As observed in Table 1, both results of TabUnite-i2bFlow and TabUnite-dicFlow achieve the best
 250 performance compared to existing baselines. We also identify that TabUnite-i2bFlow is superior to
 251 TabUnite-dicFlow as most datasets contain more non-ordinal categorical features than ordinal ones.
 252 To further justify the faithfulness of our model, we use synthetic toy examples, allowing us to assess
 253 our model’s integrity against the known ground truth.

254 4.2 Ground Truth Assessment with Synthetic Toy Examples

255 **Qualitative Results.** We further demonstrate the effectiveness of our method in identifying ground
 256 truth relevance for data synthesis. We created a synthetic “Olympic” tabular dataset and visualised
 257 it qualitatively in terms of its structure (shape and sharpness of Olympic rings) and colour. Details
 258 regarding the dataset can be found in Appendix C.1. Our goal is to illustrate the integrity of
 259 our encoding method and sampling speed by mimicking the qualitative ground truth attributes of
 260 the real dataset. Our primary predefined model for comparison is TabDDPM. We also introduce
 261 TabFlow, a replica of TabDDPM except that we replace DDPM/Multinomial Diffusion with Flow
 262 Matching/Discrete Flow Models (Campbell et al., 2024).

263 Figure 3a displays the synthesised samples for TabUnite-i2bFlow, TabUnite-dicFlow, TabFlow, and
 264 TabDDPM across various sampling steps. As early as 10 steps, both TabUnite methods converge,
 265 achieving high-quality structure and colour in relation to the ideal “Ground Truth” visualisation.
 266 However, there is no apparent “Olympic” structure for TabDDPM. Although TabFlow presents an
 267 “Olympic” structure, it is difficult to identify the colours. TabFlow requires approximately 100 steps to
 268 differentiate between the colours clearly. Even at 500 steps, TabDDPM is still lacking in terms of its
 269 structure where the rings are visually less precise when compared to the “Ground Truth”. Therefore,
 270 the experiment highlights both TabUnite-i2bFlow and TabUnite-dicFlow’s faithfulness and integrity
 271 in generating high-quality samples that match the ground truth in a short period of sampling duration.

272 **Quantitative Results.** In addition to our qualitative results, we further demonstrate quantitatively
 273 that our methods are faithful to the model’s decision-making process by creating an additional
 274 synthetic toy dataset. In this dataset, categorical columns are created through an injective mapping

Table 2: RMSE (regression), Column-Wise Density Estimation (CDE), Pair-Wise Column Correlation (PCC), α -Precision, and β -Recall scores for our Census Synthetic and Beijing datasets. \uparrow indicates that the higher the score, the better the performance, vice versa. Values bolded in red and blue are the best and second best-performing models respectively. Details are found in Appendix C.

Methods	Census Synthetic					Overall Rank
	RMSE \downarrow	CDE \uparrow	PCC \uparrow	α \uparrow	β \uparrow	
TabDDPM	0.194 \pm 0.012	86.44\pm0.011	90.29 \pm 0.109	86.60 \pm 0.104	34.37 \pm 0.050	5
oheDDPM	1.171 \pm 0.024	55.34 \pm 0.023	50.66 \pm 0.014	0.600 \pm 0.001	0.000 \pm 0.000	8
i2bDDPM	0.156 \pm 0.004	76.52 \pm 0.006	77.38 \pm 0.584	77.54 \pm 0.098	1.25 \pm 0.008	6
dicDDPM	0.168 \pm 0.005	86.55\pm0.023	90.36 \pm 0.109	91.86 \pm 0.019	34.11 \pm 0.080	4
TabFlow	0.131\pm0.005	86.12 \pm 0.007	90.07 \pm 0.704	95.31\pm0.038	39.17\pm0.098	3
oheFlow	0.332 \pm 0.003	75.57 \pm 0.011	79.58 \pm 0.189	69.59 \pm 0.080	0.241 \pm 0.015	7
TabUnite-i2bFlow	0.125\pm0.003	86.41 \pm 0.016	90.95\pm0.106	91.65 \pm 0.067	39.30\pm0.074	1
TabUnite-dicFlow	0.140 \pm 0.003	86.13 \pm 0.022	90.49\pm0.101	98.15\pm0.060	36.16 \pm 0.047	2

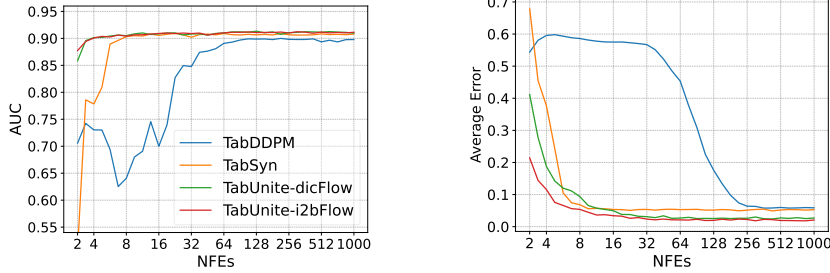
Methods	Beijing					Overall Rank
	RMSE \downarrow	CDE \uparrow	PCC \uparrow	α \uparrow	β \uparrow	
TabDDPM	1.91 \pm 0.680	66.98 \pm 22.6	61.63 \pm 24.3	33.99 \pm 46.1	19.89 \pm 24.9	7
oheDDPM	2.07 \pm 0.697	48.88 \pm 2.26	44.70 \pm 3.61	2.74 \pm 0.78	3.43 \pm 2.05	8
i2bDDPM	0.662 \pm 0.017	82.17 \pm 0.27	69.95 \pm 0.60	57.78 \pm 0.83	27.15 \pm 3.56	5
dicDDPM	0.960 \pm 0.100	84.23 \pm 1.46	69.07 \pm 2.26	74.73 \pm 12.5	12.74 \pm 3.89	6
TabFlow	0.583 \pm 0.018	96.57 \pm 0.07	94.10 \pm 0.16	96.16\pm0.95	58.43 \pm 1.22	3
oheFlow	0.741 \pm 0.017	85.45 \pm 0.98	75.39 \pm 1.96	84.98 \pm 6.39	20.45 \pm 1.71	4
TabUnite-i2bFlow	0.538\pm0.007	97.47\pm0.33	96.23\pm0.39	96.08 \pm 1.45	61.02\pm0.59	2
TabUnite-dicFlow	0.559\pm0.009	98.15\pm0.17	96.27\pm0.31	97.64\pm0.55	60.69\pm0.40	1

275 from the numerical columns. We evaluate the synthesis of these categorical variables by taking the
276 absolute value of the difference between the real value and the synthesised value. More details can
277 be found in Appendix C.1. Our result in Figure 3b depicts the accuracy of the generated categorical
278 columns over the number of training iterations. It illustrates that training both TabUnite models is
279 stable and converges at a higher accuracy when compared to TabDDPM while remaining competitive
280 with TabFlow.

281 4.3 Ablation Study: Encoding Scheme and Model Choice

282 To further validate the effectiveness of Analog Bits and Dictionary encoding schemes, as well as
283 Flow Matching as our generative model, we conduct an ablation study to isolate the generative
284 model while varying the encoding methods among Analog Bits, Dictionary, separate modelling,
285 and one-hot encoding. We also perform the reverse, isolating the encoding schemes while varying
286 the generative models between Flow Matching and DDPM. The real-world dataset we select for
287 comparison is “Beijing” since it has a good amount of samples (43,824) as well as a balanced set
288 of continuous (7) and categorical (5) features. However, an issue is that a vast majority of these
289 publicly available datasets from the UCI machine learning repository (Dua & Graff, 2017) as well as
290 other databases (Vanschoren et al., 2013) lack datasets with a large number of samples (> 100k) and
291 mixed features (> 15 continuous and categorical features). Furthermore, accessing high-dimensional
292 real-world datasets with heterogeneous features can be challenging. For instance, the PLCO dataset
293 (Gohagan et al., 2000) requires 1-4 weeks for access approval due to ethical considerations and patient
294 privacy protocols, and the MAGGIC dataset (Pocock et al., 2013) involves stringent access requests.
295 Therefore, the need for curating publicly available large datasets with mixed features remains crucial
296 for determining the effectiveness of our categorical encoding schemes.

297 **Curation of a Large-Scaled Mixed Synthetic Dataset.** A considerably larger dataset is the US
298 Census Data (1990) (Meek et al., 2001) which contains 2,458,285 samples and 61 features. However,
299 these samples consist of only categorical variables. To incorporate continuous features, we begin
300 by converting ordinal categorical features into continuous features. With the remaining non-ordinal
301 categorical features, we select a subset and convert them to continuous using Frequency Encoding.
302 Lastly, we leverage a synthetic data generation model (Chen et al., 2018; Si et al., 2023) to create
303 continuous composite indicators (OECD et al., 2008) that can help capture interactions between



(a) AUC vs. Sampling Speed (NFEs) (b) Avg. Error vs. Sampling Speed (NFEs)

Figure 4: Synthetic Data Quality vs. Sampling Speed of TabUnite (i2bFlow/dicFlow), TabSYN and TabDDPM on the Adult dataset. TabUnite converges to its best AUC/Average Error in much fewer NFEs when compared to TabSyn and TabDDPM.

304 different aspects of the data. The synthetic continuous data are then generated per the following two
 305 polynomials: $\text{Syn1} = \exp(x_i x_j)$ and $\text{Syn2} = \exp(\sum_{i=1}^3 (x_i^2 - 4))$ before applying a logistic function
 306 $\frac{1}{1 + \logit(\mathbf{X})}$. Finally, we concatenate our synthesised continuous features with the categorical. We
 307 have now constructed a Census Synthetic dataset comprised of 41 continuous features, 40 categorical
 308 features and 2,458,285 samples. For a regression task, the label is “dIncome1” which is the annual
 309 income of an individual. Further details can be found in Appendix C.1.

310 **Analysis.** As observed in Table 2, both TabUnite methods achieve the highest ranking performances
 311 in both datasets across all the benchmarks. Solely comparing the performance of our encoding
 312 methods, we observed that our “i2b{ }” ({} refers to either Flow or DDPM) and “dic{ }” encoding
 313 schemes outperform separated modelling (Tab{ }) and one-hot encoding (ohe{ }) in almost all metrics.
 314 Focusing on the “Beijing” dataset, TabUnite-dicFlow outperforms TabUnite-i2bFlow in 3/5 metrics.
 315 We hypothesise that since “Beijing” contains “combined wind direction” as an ordinal categori-
 316 cal feature, TabUnite-dicFlow should be able to outperform TabUnite-i2bFlow in several metrics
 317 depending on the feature’s importance. Within our “Census Synthetic” dataset, we observe that
 318 TabUnite-i2bFlow dominates the performance when compared to TabUnite-dicFlow. This is because
 319 “Census Synthetic” contains no ordinal categorical features after converting them to continuous ones
 320 hence, it is rational for Analog Bits to have a better performance. On the other hand, comparing the
 321 performance of the generative models (Flow Matching vs. Diffusion) i.e. []Flow methods vs []DDPM
 322 methods ([] refers to either i2b, dic, Tab or ohe), Flow Matching achieves a superior performance.
 323 Additionally, we also investigate the sampling speed of our flow-based methods against TabSyn and
 324 TabDDPM. As shown in Figure 4, we observe that TabUnite converges to its best AUC/Average Error
 325 in much fewer NFEs when compared to TabSyn and TabDDPM. Therefore, the TabUnite methods
 326 have the best sampling efficiency, followed by TabSYN and TabDDPM.

327 5 Conclusion and Limitation

328 We propose an efficient encoding framework for tabular data generation that leverages effective
 329 categorical encoding schemes to unify the data space. This enables us to apply a single generative
 330 model that captures heterogeneous feature interrelationships, improving generation quality. Our
 331 models are curated by employing Analog Bits and Dictionary encoding that efficiently convert
 332 categorical variables into a dense and compact continuous representation, before applying Conditional
 333 Flow Matching to generate the data. To further strengthen our findings on our categorical embedding
 334 schemes, we curate a large-scale heterogeneous tabular dataset. Relative to the baselines, our
 335 TabUnite models outperform them across a wide range of datasets whilst evaluated on a broad suite of
 336 benchmarks. Additionally, leveraging Flow Matching greatly bolsters our sampling efficiency, saving
 337 computational cost and time. Overall, we justify our claim of applying efficient encoding methods to
 338 enable the application of a single/unified generative model on a coherent data space. A limitation of
 339 our methodology is that we have not extensively explored a continuous embedding scheme where we
 340 perform the reverse and unify the generative space into a categorical one. Inspired by (Ansari et al.,
 341 2024), we conduct initial explorations of time series tokenization to embed continuous features yet,
 342 our results are still inconclusive and left to future work.

343 References

- 344 Alaa, A. M., van Breugel, B., Saveliev, E., and van der Schaar, M. How faithful is your synthetic
345 data? sample-level metrics for evaluating and auditing generative models, 2022.
- 346 Ansari, A. F., Stella, L., Turkmen, C., Zhang, X., Mercado, P., Shen, H., Shchur, O., Rangapuram,
347 S. S., Arango, S. P., Kapoor, S., Zschiegner, J., Maddix, D. C., Wang, H., Mahoney, M. W.,
348 Torkkola, K., Wilson, A. G., Bohlke-Schneider, M., and Wang, Y. Chronos: Learning the language
349 of time series, 2024.
- 350 Becker, B. and Kohavi, R. Adult. UCI Machine Learning Repository, 1996. DOI:
351 <https://doi.org/10.24432/C5XW20>.
- 352 Borisov, V., Seßler, K., Leemann, T., Pawelczyk, M., and Kasneci, G. Language models are realistic
353 tabular data generators, 2023.
- 354 Campbell, A., Yim, J., Barzilay, R., Rainforth, T., and Jaakkola, T. Generative flows on discrete
355 state-spaces: Enabling multimodal flows with applications to protein co-design, 2024.
- 356 Chawla, N. V., Bowyer, K. W., Hall, L. O., and Kegelmeyer, W. P. Smote: Synthetic minority
357 over-sampling technique. *Journal of Artificial Intelligence Research*, 16:321–357, June 2002.
358 ISSN 1076-9757. doi: 10.1613/jair.953. URL <http://dx.doi.org/10.1613/jair.953>.
- 359 Chen, J., Song, L., Wainwright, M. J., and Jordan, M. I. Learning to explain: An information-theoretic
360 perspective on model interpretation, 2018.
- 361 Chen, R. T. Q., Rubanova, Y., Bettencourt, J., and Duvenaud, D. Neural ordinary differential
362 equations, 2019.
- 363 Chen, T. and Guestrin, C. Xgboost: A scalable tree boosting system. In *Proceedings of the 22nd ACM*
364 *SIGKDD International Conference on Knowledge Discovery and Data Mining*, KDD '16. ACM,
365 August 2016. doi: 10.1145/2939672.2939785. URL [http://dx.doi.org/10.1145/2939672.](http://dx.doi.org/10.1145/2939672.2939785)
366 [2939785](http://dx.doi.org/10.1145/2939672.2939785).
- 367 Chen, T., Kornblith, S., Norouzi, M., and Hinton, G. A simple framework for contrastive learning of
368 visual representations, 2020.
- 369 Chen, T., Zhang, R., and Hinton, G. Analog bits: Generating discrete data using diffusion models
370 with self-conditioning. *arXiv preprint arXiv:2208.04202*, 2022.
- 371 Clore, J., Cios, K., DeShazo, J., and Strack, B. Diabetes 130-US hospitals for years 1999-2008. UCI
372 Machine Learning Repository, 2014. DOI: <https://doi.org/10.24432/C5230J>.
- 373 Datta, A. Us health insurance dataset, Feb 2020. URL [https://www.kaggle.com/datasets/](https://www.kaggle.com/datasets/teertha/ushealthinsurancedataset)
374 [teertha/ushealthinsurancedataset](https://www.kaggle.com/datasets/teertha/ushealthinsurancedataset).
- 375 Dua, D. and Graff, C. Uci machine learning repository, 2017. URL [http://archive.ics.uci.](http://archive.ics.uci.edu/ml)
376 [edu/ml](http://archive.ics.uci.edu/ml).
- 377 Gohagan, J. K., Prorok, P. C., Hayes, R. B., Kramer, B. S., Prostate, Lung, C., and Team, O. C. S.
378 T. P. The prostate, lung, colorectal and ovarian (plco) cancer screening trial of the national cancer
379 institute: history, organization, and status. *Control Clin Trials*, 21(6 Suppl):251S–272S, Dec 2000.
380 doi: 10.1016/s0197-2456(00)00097-0.
- 381 Goodfellow, I. J., Pouget-Abadie, J., Mirza, M., Xu, B., Warde-Farley, D., Ozair, S., Courville, A.,
382 and Bengio, Y. Generative adversarial networks, 2014.
- 383 Gorishniy, Y., Rubachev, I., Khrulkov, V., and Babenko, A. Revisiting deep learning models for
384 tabular data, 2023.
- 385 He, K., Zhang, X., Ren, S., and Sun, J. Deep residual learning for image recognition, 2015.
- 386 Higgins, I., Matthey, L., Pal, A., Burgess, C., Glorot, X., Botvinick, M., Mohamed, S., and Lerchner,
387 A. beta-VAE: Learning basic visual concepts with a constrained variational framework. In
388 *International Conference on Learning Representations*, 2017. URL [https://openreview.net/](https://openreview.net/forum?id=Sy2fzU9g1)
389 [forum?id=Sy2fzU9g1](https://openreview.net/forum?id=Sy2fzU9g1).

- 390 Ho, J., Jain, A., and Abbeel, P. Denoising diffusion probabilistic models. *Advances in neural*
391 *information processing systems*, 33:6840–6851, 2020.
- 392 Hooeboom, E., Nielsen, D., Jaini, P., Forré, P., and Welling, M. Argmax flows and multinomial
393 diffusion: Learning categorical distributions, 2021.
- 394 Jolicoeur-Martineau, A., Fatras, K., and Kachman, T. Generating and imputing tabular data via
395 diffusion and flow-based gradient-boosted trees, 2024.
- 396 Karras, T., Aittala, M., Aila, T., and Laine, S. Elucidating the design space of diffusion-based
397 generative models, 2022.
- 398 Kim, J., Lee, C., and Park, N. Stasy: Score-based tabular data synthesis. *arXiv preprint*
399 *arXiv:2210.04018*, 2022.
- 400 Kingma, D. P. and Ba, J. Adam: A method for stochastic optimization. *arXiv preprint*
401 *arXiv:1412.6980*, 2014.
- 402 Kingma, D. P. and Welling, M. Auto-encoding variational bayes. *arXiv preprint arXiv:1312.6114*,
403 2013.
- 404 Kotelnikov, A., Baranchuk, D., Rubachev, I., and Babenko, A. Tabddpm: Modelling tabular data with
405 diffusion models. In *International Conference on Machine Learning*, pp. 17564–17579. PMLR,
406 2023.
- 407 Krishnan, R. G., Liang, D., and Hoffman, M. On the challenges of learning with inference networks
408 on sparse, high-dimensional data, 2017.
- 409 Lee, C., Kim, J., and Park, N. Codi: Co-evolving contrastive diffusion models for mixed-type tabular
410 synthesis. In *International Conference on Machine Learning*, pp. 18940–18956. PMLR, 2023.
- 411 Lipman, Y., Chen, R. T., Ben-Hamu, H., Nickel, M., and Le, M. Flow matching for generative
412 modeling. *arXiv preprint arXiv:2210.02747*, 2022.
- 413 Liu, T., Qian, Z., Berrevoets, J., and van der Schaar, M. GOGGLE: Generative modelling for
414 tabular data by learning relational structure. In *The Eleventh International Conference on Learning*
415 *Representations*, 2023. URL <https://openreview.net/forum?id=fPVRcJqspu>.
- 416 Liu, X., Gong, C., and Liu, Q. Flow straight and fast: Learning to generate and transfer data with
417 rectified flow. *arXiv preprint arXiv:2209.03003*, 2022.
- 418 Mairal, J., Ponce, J., Sapiro, G., Zisserman, A., and Bach, F. Supervised dictionary learning. In Koller,
419 D., Schuurmans, D., Bengio, Y., and Bottou, L. (eds.), *Advances in Neural Information Processing*
420 *Systems*, volume 21. Curran Associates, Inc., 2008. URL [https://proceedings.neurips.cc/
421 paper_files/paper/2008/file/c0f168ce8900fa56e57789e2a2f2c9d0-Paper.pdf](https://proceedings.neurips.cc/paper_files/paper/2008/file/c0f168ce8900fa56e57789e2a2f2c9d0-Paper.pdf).
- 422 Mairal, J., Bach, F., Ponce, J., and Sapiro, G. Online dictionary learning for sparse coding. In *Proceed-*
423 *ings of the 26th Annual International Conference on Machine Learning, ICML '09*, pp. 689–696,
424 New York, NY, USA, 2009. Association for Computing Machinery. ISBN 9781605585161. doi:
425 10.1145/1553374.1553463. URL <https://doi.org/10.1145/1553374.1553463>.
- 426 McCann, R. J. A convexity principle for interacting gases. *Advances in Mathematics*, 128(1):
427 153–179, 1997. ISSN 0001-8708. doi: <https://doi.org/10.1006/aima.1997.1634>. URL <https://www.sciencedirect.com/science/article/pii/S0001870897916340>.
- 429 Meek, C., Thiesson, B., and Heckerman, D. US Census Data (1990). UCI Machine Learning
430 Repository, 2001. DOI: <https://doi.org/10.24432/C5VP42>.
- 431 Minieri, A. Synthetic data for privacy preservation - part 2. [https://www.clearbox.ai/blog/
432 2022-06-07-synthetic-data-for-privacy-preservation-part-2](https://www.clearbox.ai/blog/2022-06-07-synthetic-data-for-privacy-preservation-part-2), 2022. Accessed:
433 2024-05-20.
- 434 Moro, S., Rita, P., and Cortez, P. Bank Marketing. UCI Machine Learning Repository, 2012. DOI:
435 <https://doi.org/10.24432/C5K306>.

- 436 OECD, Union, E., and European Commission, J. R. C. *Handbook on Constructing Composite*
437 *Indicators: Methodology and User Guide*. OECD Publishing, 2008. doi: [https://doi.org/10.](https://doi.org/10.1787/9789264043466-en)
438 [1787/9789264043466-en](https://doi.org/10.1787/9789264043466-en). URL [https://www.oecd-ilibrary.org/content/publication/](https://www.oecd-ilibrary.org/content/publication/9789264043466-en)
439 [9789264043466-en](https://www.oecd-ilibrary.org/content/publication/9789264043466-en).
- 440 Onishi, S. and Meguro, S. Rethinking data augmentation for tabular data in deep learning. *arXiv*
441 *preprint arXiv:2305.10308*, 2023.
- 442 Pedregosa, F., Varoquaux, G., Gramfort, A., Michel, V., Thirion, B., Grisel, O., Blondel, M.,
443 Prettenhofer, P., Weiss, R., Dubourg, V., Vanderplas, J., Passos, A., Cournapeau, D., Brucher, M.,
444 Perrot, M., and Duchesnay, E. Scikit-learn: Machine learning in Python. *Journal of Machine*
445 *Learning Research*, 12:2825–2830, 2011.
- 446 Pocock, S. J., Ariti, C. A., McMurray, J. J. V., Maggioni, A., Køber, L., Squire, I. B., Swedberg, K.,
447 Dobson, J., Poppe, K. K., Whalley, G. A., Doughty, R. N., and in Chronic Heart Failure, M.-A.
448 G. G. Predicting survival in heart failure: a risk score based on 39 372 patients from 30 studies.
449 *European Heart Journal*, 34(19):1404–1413, May 2013. doi: 10.1093/eurheartj/ehs337.
- 450 Poslavskaya, E. and Korolev, A. Encoding categorical data: Is there yet anything 'hotter' than one-hot
451 encoding?, 2023.
- 452 Rabaey, P., Deleu, J., Heytens, S., and Demeester, T. Clinical reasoning over tabular data and text
453 with bayesian networks. *arXiv preprint arXiv:2403.09481*, 2024.
- 454 Rezende, D. J. and Mohamed, S. Variational inference with normalizing flows, 2016.
- 455 Sauber-Cole, R. and Khoshgoftaar, T. M. The use of generative adversarial networks to alleviate
456 class imbalance in tabular data: a survey. *Journal of Big Data*, 9(1):98, 2022.
- 457 SDMetrics. Detection metrics (single table) - sdmetrics documentation, 2024. URL [https://docs.](https://docs.sdv.dev/sdmetrics/metrics/metrics-in-beta/detection-single-table)
458 [sdv.dev/sdmetrics/metrics/metrics-in-beta/detection-single-table](https://docs.sdv.dev/sdmetrics/metrics/metrics-in-beta/detection-single-table). Accessed:
459 2024-05-20.
- 460 Sennrich, R., Haddow, B., and Birch, A. Neural machine translation of rare words with subword
461 units, 2016.
- 462 Si, J. Y. H., Cooper, M., Cheng, W. Y., and Krishnan, R. Interpretabnet: Enhancing interpretability of
463 tabular data using deep generative models and large language models. In *NeurIPS 2023 Second*
464 *Table Representation Learning Workshop*, 2023. URL [https://openreview.net/forum?id=](https://openreview.net/forum?id=kzR5Cj5b1w)
465 [kzR5Cj5b1w](https://openreview.net/forum?id=kzR5Cj5b1w).
- 466 Song, J., Meng, C., and Ermon, S. Denoising diffusion implicit models, 2022.
- 467 Song, Y., Sohl-Dickstein, J., Kingma, D. P., Kumar, A., Ermon, S., and Poole, B. Score-based
468 generative modeling through stochastic differential equations, 2021.
- 469 Tong, A., Malkin, N., Huguet, G., Zhang, Y., Rector-Brooks, J., Fatras, K., Wolf, G., and Bengio, Y.
470 Improving and generalizing flow-based generative models with minibatch optimal transport. In
471 *ICML Workshop on New Frontiers in Learning, Control, and Dynamical Systems*, 2023.
- 472 van Breugel, B. and van der Schaar, M. Why tabular foundation models should be a research priority,
473 2024.
- 474 Vanschoren, J., van Rijn, J. N., Bischl, B., and Torgo, L. Openml: networked science in machine
475 learning. *SIGKDD Explorations*, 15(2):49–60, 2013. doi: 10.1145/2641190.2641198. URL
476 <http://doi.acm.org/10.1145/2641190.2641198>.
- 477 Xu, L., Skoularidou, M., Cuesta-Infante, A., and Veeramachaneni, K. Modeling tabular data using
478 conditional gan, 2019.
- 479 Yoon, J., Jordon, J., and van der Schaar, M. INVASE: Instance-wise variable selection using
480 neural networks. In *International Conference on Learning Representations*, 2019. URL [https:](https://openreview.net/forum?id=BJg_roAcK7)
481 [//openreview.net/forum?id=BJg_roAcK7](https://openreview.net/forum?id=BJg_roAcK7).
- 482 Zhang, H., Zhang, J., Srinivasan, B., Shen, Z., Qin, X., Faloutsos, C., Rangwala, H., and Karypis,
483 G. Mixed-type tabular data synthesis with score-based diffusion in latent space. *arXiv preprint*
484 *arXiv:2310.09656*, 2023.

Appendix

485

486 Contents

487	A Algorithms	14
488	B Architecture	15
489	B.1 Flow Matching MLP	15
490	B.2 Hyperparameters	15
491	C Experimental Details	16
492	C.1 Datasets	16
493	C.2 Additional Details on Baselines: Predefined Models.	19
494	C.3 Additional Details on Ablations: Encoding schemes and generative models (Flow/Diffusion).	19
495	C.4 Benchmarks	21
496	D Further Experimental Results	24
497	D.1 Training and Sampling Time	24
498	D.2 Low-order statistics: Column-wise density estimation and Pair-wise column correlation	24
499	D.3 High-order metrics: Alpha-precision and Beta-recall	25
500	D.4 Detection metric: Classifier Two-Sample Test (C2ST)	26
501	D.5 Privacy metric: Distance to Closest Record	26

502 **A Algorithms**

503 Algorithms 1 and 2 describe the training and sampling Flow Matching process of TabUnite. For more
504 information regarding Flow Matching, please refer to “Flow Matching for Generative Modeling”
505 (Lipman et al., 2022) or “Improving and Generalizing Flow-Based Generative Models with Minibatch
506 Optimal Transport” (Tong et al., 2023).

Algorithm 1 TabUnite: Training Flow Matching using CFM

- 1: Sample initial data points $\mathbf{x}_1 \sim q(\mathbf{x}_1)$
 - 2: Initialize vector field $v_t(\mathbf{x})$ and parameters θ
 - 3: **while** not converged **do**
 - 4: Sample time step $t \sim U([0, 1])$
 - 5: Sample $\mathbf{x} \sim p_t(\mathbf{x}|\mathbf{x}_1)$
 - 6: Calculate true vector field $u_t(\mathbf{x}|\mathbf{x}_1)$ as per Eq. 3
 - 7: Compute loss $L_{CFM}(\theta) = \mathbb{E}|v_t(\mathbf{x}) - u_t(\mathbf{x}|\mathbf{x}_1)|^2$
 - 8: Update θ using gradient descent to minimize $L_{CFM}(\theta)$
 - 9: **end while**
-

Algorithm 2 TabUnite: Sampling Flow Matching using CFM

- 1: Sample $\mathbf{x} \sim \mathcal{N}(\mathbf{0}, \mathbf{I})$ (start with the noise distribution)
 - 2: Set $t_{\max} = T$ and initialize $\mathbf{x}_T = \mathbf{x}$
 - 3: **for** $i = T, \dots, 1$ **do**
 - 4: Use ψ_t to map \mathbf{x}_T to $\mathbf{x}_{t_{i-1}}$ using the learned vector field u_t
 - 5: Compute $\mathbf{x}_{t_{i-1}}$ with $\psi_{t_i}(\mathbf{x}_T) = \sigma_{t_i}(\mathbf{x}_1)\mathbf{x}_T + \mu_{t_i}(\mathbf{x}_1)$
 - 6: Update $\mathbf{x}_T = \mathbf{x}_{t_{i-1}}$
 - 7: **end for**
 - 8: \mathbf{x}_0 is a synthetic sample generated by CFM
-

507 **B Architecture**

508 **B.1 Flow Matching MLP**

509 Figure 5 illustrates the MLP architecture used as part of our Flow Matching network, also used in
 510 TabDDPM (Kotelnikov et al., 2023) and TabSYN (Zhang et al., 2023), which is based on Gorishniy
 511 et al. (2023).

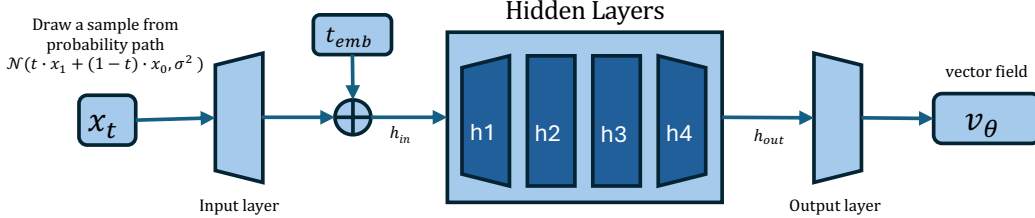


Figure 5: The MLP architecture used in the Flow Matching process. The neural network takes in a batch of samples drawn from the probability path at time t 's sampled from $\mathcal{U}(0, 1)$ to create a vector field v_θ that represents a continuous normalizing flow from pure noise to our data distribution $p_1(x_1)$.

512 The input layer projects the batch of tabular data input samples x_t , each with dimension d_{in} , to the
 513 dimensionality d_t of our time step embeddings t_{emb} through a fully connected layer. This is so that
 514 we may leverage temporal information, which is appended to the result of the projection in the form
 515 of sinusoidal time step embeddings.

$$h_{in} = FC_{d_t}(x_t) + t_{emb} \quad (5)$$

516 The hidden layers h_1, h_2, h_3 , and h_4 are fully connected networks used to learn and create the vector
 517 field. The output dimension of each layer is chosen as $d_t, 2d_t, 2d_t$, and d_t respectively. On top of the
 518 FC networks, each layer also consists of an activation function followed by dropout, as seen in the
 519 formulas below. This formulation is repeated for each hidden layer, at the end of which we obtain
 520 h_{out} . The exact activations, dropout, and other hyperparameters chosen are shown in Table 3.

$$h_1 = Dropout(Activation(FC(h_{in}))) \quad (6)$$

521 At last, the output layer transforms h_{out} , of dimension d_{emb} back to dimension d_{in} through a fully
 522 connected network, which now represents the vector field v_θ .

$$v_\theta = FC_{d_{in}}(h_{out}) \quad (7)$$

523 **B.2 Hyperparameters**

524 We generally utilise the same hyperparameters as TabSYN (Zhang et al., 2023) and TabDDPM
 525 (Kotelnikov et al., 2023) for comparability. The exact hyperparameters selected for our models are
 526 shown below in Table 3.

Table 3: TabUnite Hyperparameters.

General		Flow Matching MLP	
Hyperparameter	Value	Hyperparameter	Value
Training Iterations	100,000	Timestep embedding dimension d_t	1024
Flow Matching Timesteps	1,000	Activation	ReLU
Learning Rate	$1e-4$	Dropout	0.0
Weight Decay	$5e-4$	Hidden layer dimension $[h_1, h_2, h_3, h_4]$	[1024, 2048, 2048, 1024]
Batch Size	4096		

527 C Experimental Details

528 The following delineates the foundation of our experiments:

- 529 • Codebase: Python & PyTorch
- 530 • GPU: Nvidia RTX 3090, 24GB VRAM
- 531 • Optimizer: Adam (Kingma & Ba, 2014)

532 Experiment Table Details

533 For Tables 1 and 2, the Overall Rank is calculated by first ranking them individually within each
534 benchmark (row-wise), then averaging their ranks for each method across the benchmarks (column-
535 wise), before rounding the ranks to the nearest integer.

536 In Table 1 and Appendix Tables, all reported results of baselines in our experiments are taken from
537 Zhang et al. (2023), except for TabSYN and TabDDPM, whose results are reproduced utilising the
538 public repository: <https://github.com/amazon-science/tabsyn>. Additionally, for Table 1,
539 we decided to rerun GReaT in the same original setting (1 Train, 20 Samples) for the Adult dataset
540 as TabSYN’s reported results (0.913 ± 0.003) were unusually high. All reported results follow
541 TabSYN’s 1 Training and 20 Sampling trial setting. Note that TabDDPM collapses on the News
542 dataset for all the benchmarks.

543 In Table 2, we limit ourselves to only one real-world dataset + our curated “Census Synthetic” dataset.
544 Additionally, we computed 1 Training and 3 Sampling trials for our error bars. Lastly, Pair-Wise
545 Column Correlation for the “Census Synthetic” dataset is evaluated on a 10% subsample. These
546 reasons are due to the fact that it is computationally costly to compute results for the diffusion-based
547 models.

548 C.1 Datasets

549 Real World Datasets

550 Experiments were conducted with a total of 6 tabular datasets from the UCI Machine Learning
551 Repository (Dua & Graff, 2017) with a (CC-BY 4.0) license. Classification tasks were performed on
552 the Adult, Default, Magic, and Shoppers datasets, while regression tasks were performed on the
553 Beijing and News datasets. Each dataset was split into training, validation, and testing sets with a
554 ratio of 8:1:1, except for the Adult dataset, whose official testing set was used and the remainder
555 split into training and validation sets with an 8:1 ratio. The resulting statistics of each dataset are
556 shown below in Table 4. Note that the target column indicates the specific operation applied to each
557 dataset: binary classification for a categorical target with two classes, multiclass classification for a
558 categorical target with more than two classes, and regression for a numerical target feature. Some
detailed information as well as the statistics of the datasets are shown in Tables 4 and 5 respectively.

Table 4: Statistics of datasets. "# Num" stands for the number of numerical columns, and "# Cat" stands for the number of categorical columns.

Dataset	# Rows	# Num	# Cat	# Train	# Validation	# Test	Task Type
Adult	48,842	6	9	28,943	3,618	16,281	Binary Classification
Default	30,000	14	11	24,000	3,000	3,000	Binary Classification
Shoppers	12,330	10	8	9,864	1,233	1,233	Binary Classification
Magic	19,019	10	1	15,215	1,902	1,902	Binary Classification
Beijing	43,824	7	5	35,058	4,383	4,383	Regression
News	39,644	46	2	31,714	3,965	3,965	Regression
Census Synthetic	2,458,285	41	40	1,966,621	245,827	245,829	Regression

559

560 Synthetic Toy Datasets

561 *Qualitative Toy Dataset:* The dataset consists of four columns, with the first two columns representing
562 numerical data point coordinates. Subsequently, the third column categorizes the data points into
563 five circles whereas the last column indicates the 5 colours each data point can be classified into.

Table 5: Details of datasets. The "Feature Information" column details the contents of the dataset and how it is curated. The "Prediction Task" column describes the model’s objective on that dataset.

Dataset	Feature Information	Prediction Task
Adult	Demographic and occupational variables from census data	Whether an individual’s income exceeds \$50,000
Default	Demographic and account-specific data collected from credit card clients	Whether an individual will default on their credit card payments next month
Shoppers	Internet users’ browser session information	Whether the user will engage in online shopping
Magic	Generated events simulating the imaging of gamma-ray air showers	Predict the type of high-energy gamma particles in the atmosphere
Beijing	Hourly atmospheric PM2.5 and meteorological data readings at the U.S. Embassy in Beijing	Predict future PM2.5 readings
News	Various features from the news site Mashable’s published articles	The number of "shares" articles will have on social media
Census Synthetic	1990 Census Demographics of the US Population	Annual Income of an individual

564 Therefore, each row in the dataset contains 2 numerical features and 2 categorical features. A total of
565 10, 000 samples are generated for this dataset.

566 *Quantitative Toy Dataset:* To quantify our model’s ability to generate high-quality data, we generate
567 a synthetic toy dataset with 11 numerical features, all drawn from a unit Gaussian distribution, to
568 represent a complex underlying data distribution. From these numerical features, we derive six
569 categorical variables by applying a variety of transformations, the details of which are described by
570 the equations below.

571

$$\begin{aligned}
x_1^{cat} &= x_0^{num} \cdot x_1^{num} \\
x_2^{cat} &= (x_2^{num})^2 + (x_3^{num})^2 + (x_4^{num})^2 + (x_5^{num})^2 - 4 \\
x_3^{cat} &= -10 \cdot \sin(2 \cdot x_6^{num}) + 2 \cdot |x_7^{num}| + x_8^{num} - e^{-x_9^{num}} \\
x_4^{cat} &= (x_9^{num} < 0) \cdot x_1^{cat} + (1 - (x_9^{num} < 0)) \cdot x_2^{cat} \\
x_5^{cat} &= (x_9^{num} < 0) \cdot x_1^{cat} + (1 - (x_9^{num} < 0)) \cdot x_3^{cat} \\
x_6^{cat} &= (x_9^{num} < 0) \cdot x_2^{cat} + (1 - (x_9^{num} < 0)) \cdot x_3^{cat}
\end{aligned} \tag{8}$$

572 Following the transformations, tanh activation functions are applied followed by digitization to 10
573 separate bins. A total of 10, 000 samples are generated for this dataset, resulting in our discrete
574 categorical variables. We quantify the performance of our models by examining the fidelity of
575 generating these categorical variables. The scoring is determined by taking the absolute value of the
576 difference between the real and synthesized values.

577 We perform three trial experiments for each method and report their mean and standard deviation.
578 Note that in the quantitative experiments, we use a DDIM sampler for TabDDPM thus, the results are
579 slightly worse than those we reported in our previous tables.

580 Census Synthetic Dataset

581 The US Census Data (1990) (Meek et al., 2001) ((CC-BY 4.0) license) contains 2, 458, 285 samples
582 and 61 features (excluding “dIncome2” to “dIncome8” since they are redundant). However, these
583 samples consist of only categorical variables. To incorporate continuous features, we begin by
584 converting the following ordinal categorical features into continuous features:

- 585 • Annual income: dIncome1
- 586 • Earnings from employment: dRearning
- 587 • Age: dAge

- 588 • English proficiency: iEnglish
- 589 • Hours worked in 1989: dHour89
- 590 • Hours worked per week: dHours
- 591 • Travel time to work: dTravtime
- 592 • Years spent schooling: iYearsch
- 593 • Years spent working: iYearwrk

594 A total of 9 ordinal categorical features are converted. With the remaining non-ordinal categorical
 595 features, we select 12 additional categorical features and convert them to continuous using Frequency
 596 Encoding yielding us 21 continuous features in total. We consider features that are likely to have
 597 a variety of categories and could benefit from a frequency-based transformation. For instance,
 598 occupation covers a wide range of jobs and ancestry covers many different backgrounds. The features
 599 are as follows:

- 600 • Primary ancestry: dAncestry1
- 601 • Secondary ancestry: dAncestry2
- 602 • Citizenship status: iCitizen
- 603 • Marital status: iMarital
- 604 • Hispanic origin: dHispanic
- 605 • Class of worker: iClass
- 606 • Place of birth: dPOB
- 607 • Occupation: dOccup
- 608 • Industry: dIndustry
- 609 • Mobility status: iMobility
- 610 • Relationship to head of household: iRelat1
- 611 • Sex: iSex

612 Lastly, to balance out the remaining categorical features 40 with the 21 continuous ones, we leverage
 613 a synthetic data generation model (Chen et al., 2018; Yoon et al., 2019; Si et al., 2023) to generate
 614 20 more continuous features based on the converted continuous features. We create continuous
 615 composite indicators (OECD et al., 2008) by combining our curated continuous features in sets of 2
 616 or 3 that can help capture interactions and relationships between different aspects of the data. An
 617 example is a gender and earnings indicator that shows income disparities. Here are the composite
 618 indicators:

- 619 • Work hours (Hours worked per week and Hours worked in 1989): dHours, dHour89
- 620 • Educational attainment with age (Age and Years of schooling): dAge, iYearsch
- 621 • Language skills based on birthplace (English proficiency and Place of birth): iEnglish, dPOB
- 622 • Demographic relationships (Citizenship status and Hispanic origin): iCitizen, dHispanic
- 623 • Commuting patterns (Travel time to work and Years worked): dTravtime, iYearwrk
- 624 • Family structure (Marital status and Relationship to household head): iMarital, iRelat1
- 625 • Employment characteristics (Industry and Occupation): dIndustry, dOccup
- 626 • Income disparities (Gender and Earnings): iSex, dRearning
- 627 • Migration patterns (Mobility status and Citizenship): iMobility, iCitizen
- 628 • Heritage (Primary and Secondary Ancestry): dAncestry1, dAncestry2
- 629 • Career dedication (Hours worked per week, Hours worked in 1989, and Travel time to work):
 630 dHours, dHour89, dTravtime
- 631 • Career progression (Age, years of schooling, and years worked): dAge, iYearsch, iYearwrk
- 632 • Cultural integration (English proficiency, place of birth, and citizenship): iEnglish, dPOB,
 633 iCitizen

- 634 • Household dynamics (Marital status, relationship to household head, and mobility status):
635 iMarital, iRelat1, iMobility
- 636 • Job characteristics (Industry, Occupation, and Earnings): dIndustry, dOccup, dRearning
- 637 • Income trends (Gender, Earnings, and Age): iSex, dRearning, dAge
- 638 • Heritage and immigration status (Primary and Secondary heritage, and Citizenship):
639 dAncestry1, dAncestry2, iCitizen
- 640 • Demographic patterns (Hispanic origin, Relationship to household head, and Age): dHis-
641 panic, iRelat1, dAge
- 642 • Job location and stability (Travel time, Years worked, and Occupation): dTravtime, iYearwrk,
643 dOccup
- 644 • Education’s impact on earnings (Years of schooling, Years worked, and Earnings): iYearsch,
645 iYearwrk, dRearning

646 Before generating these composite indicators, we first apply a Standard scaler to the converted
647 continuous features since the input features are "generated from a Gaussian distribution ($X \sim$
648 $N(0, I)$)" (per (Chen et al., 2018)). The synthetic continuous data are then generated according to
649 the following two polynomials:

$$650 \quad \bullet \text{Syn1} = \exp(\mathbf{X}_i \mathbf{X}_j)$$

$$651 \quad \bullet \text{Syn2} = \exp(\sum_{i=1}^3 (\mathbf{X}_i^2 - 4))$$

652 where the first set consists of 10 indicators derived from pairs of variables following Syn1 and
653 the second set consists of 10 indicators derived from triples of variables following Syn2. These
654 composite indicators are then transformed using the logistic function $\frac{1}{1+\exp(-X)}$. Finally, we merge
655 our continuous features with the categorical features to create a comprehensive “Census Synthetic”
656 dataset. The “Census Synthetic” dataset we construct comprises of 41 continuous features, 40
657 categorical features and 2, 458, 285 samples. For a regression task, the label is “dIncome1” which is
658 the Annual income of an individual. Note that the dataset will be released with a CC-BY 4.0 license.

659 C.2 Additional Details on Baselines: Predefined Models.

660 TabUnite’s performance is evaluated in comparison to previous works in mixed-type tabular data
661 generation. This includes CTGAN and TVAE (Xu et al., 2019), GOGGLE (Liu et al., 2023), GReaT
662 (Borisov et al., 2023), STaSy (Kim et al., 2022), CoDi (Lee et al., 2023), TabDDPM (Kotelnikov
663 et al., 2023), and TabSYN (Zhang et al., 2023). The underlying architectures and implementation
664 details of these models are presented below in Table 7.

665 C.3 Additional Details on Ablations: Encoding schemes and generative models 666 (Flow/Diffusion).

667 On top of the models developed by previous related works in mixed-type tabular data synthesis, we
668 developed baselines that would provide a direct and analogous comparison to justify flow-matching
669 and our particular encoding methods. This includes the flow-matching-based one-hotFlow (oheFlow),
670 TabFlow, and the DDPM-based i2bDDPM, dicDDPM, and one-hotDDPM (oheDDPM).

671 Our DDPM-based baseline methods (i2bDDPM, dicDDPM, and oheDDPM) primarily inherit the
672 design and implementation of TabDDPM (Kotelnikov et al., 2023). Whereas TabDDPM leverages
673 two separate diffusion models, namely Gaussian diffusion and Multinomial diffusion, we devise
674 i2bDDPM, dicDDPM, and oheDDPM to rely solely on Gaussian Diffusion. This is because their
675 corresponding methods of Analog Bits, Dictionary Encoding, and One-Hot Encoding allow us
676 to perform diffusion in a unified data space. Implementation of these methods is done by simply
677 altering the data processing stage of the model. The DDPM architecture is largely kept the same.
678

679 Our Flow-based baseline methods (oheFlow, TabFlow) are extended from the TabUnite architecture,
680 which consists of i2bFlow and dicFlow. oheFlow, as the name suggests, utilizes One-Hot Encoding
681 in its data processing stage. Tabflow, on the other hand, mirrors the idea of TabDDPM in that two
682 separate models are used: one for learning categorical features and the other for learning numerical

Table 7: Comparison of previous methods in Tabular Data Synthesis.

Method	Model ¹	Type ²	Categorical Encoding	Numerical Encoding	Additional Techniques
CTGAN	GAN	U	One-Hot Encoding	Scaled Bayesian Gaussian Mixture	Mode-specific normalization to represent complex distributions & conditional generation to address data imbalances
TVAE	VAE	U	One-Hot Encoding	Scaled Bayesian Gaussian Mixture	Mode-specific normalization & conditional generation
GOGGLE	VAE + GNN	U	One-Hot Encoding	-	Learning relational structures among features graphically through an adjacency matrix
GReaT	Autoregressive GPT	U	Byte-Pair Encoding ³	Byte-Pair Encoding ³	Textual Encoder which converts data into natural language, followed by Feature Order Permutation and Fine-tuning
STaSy	Score-based Diffusion	U	One-Hot Encoding	Min-max scaler	Self-paced learning and fine-tuning
CoDi	DDPM/Multinomial Diffusion	S	One-Hot Encoding	Min-max scaler	Model Inter-conditioning and Contrastive learning to learn dependencies between categorical and numerical data
TabDDPM	DDPM/Multinomial Diffusion	S	One-Hot Encoding	Quantile Transformer	Concatenation of numerical and categorical features
TabSYN	VAE + EDM	U	One-Hot	Quantile Transformer	Feature Tokenizer and Transformer encoder to learn cross-feature relationships with adaptive loss weighing to increase reconstruction performance
TabUnite-i2BFlow	Flow Matching	U	Analog Bits	Quantile Transformer	Concatenation of numerical and categorical features encoded with TabUnite’s embedding scheme
TabUnite-dicFlow	Flow Matching	U	Dictionary	Quantile Transformer	Concatenation of numerical and categorical features encoded with TabUnite’s embedding scheme

¹ The 'Model' Column indicates the underlying architecture used for the model. Options include Generative Adversarial Networks or GANs (Goodfellow et al., 2014), Variational Autoencoders or VAEs (Kingma & Welling, 2013), Denoising Diffusion Probabilistic Models or DDPMs (Ho et al., 2020), Multinomial Diffusion (Hoogeboom et al., 2021), EDM, as introduced in Karras et al. (2022).

² The 'Type' column indicates the data integration approach used in the model. 'U' denotes a unified data space where numerical and categorical data are combined after initial processing and fed collectively into the model. 'S' represents a separated data space, where numerical and categorical data are processed and fed into distinct models.

³ Byte-Pair Encoding (Sennrich et al., 2016) is a tokenization method that iteratively merges the most frequent adjacent characters or character pairs into single tokens, creating a vocabulary of subwords that efficiently handles rare and unknown words in text processing.

683 features. Here, the implementation combines ordinary Flow Matching (Lipman et al., 2022) with
 684 Discrete Flow Matching (Campbell et al., 2024). The respective results of these two models are
 685 concatenated afterward to allow for the synthesis of mixed-type tabular data.
 686

687 These methods all utilize the QuantileTransformer (Pedregosa et al., 2011) to process numerical data,
 688 which normalizes features to follow a uniform or normal distribution. This is done through sorting
 689 and ranking data points, and then mapping them to fit to the target distribution.

690 C.4 Benchmarks

691 In this section, we expand on the concrete formulations behind our benchmarks including machine
 692 learning efficiency, low-order statistics, and high-order metrics. We also provide an overview on the
 693 detection and privacy metrics used in our experiments. These comprehensive benchmarks as well as
 694 their implementations are identical to those established by TabSYN (Zhang et al., 2023), ensuring a
 695 direct and accurate comparison.

696 Machine Learning Efficiency

697 *AUC* (Area Under Curve) is used to evaluate the efficiency of our model in binary classification tasks.
 698 It measures the area under the Receiver Operating Characteristic (or ROC) curve, which plots the
 699 True Positive Rate against the False Positive Rate. *AUC* may take values in the range $[0,1]$. A higher
 700 *AUC* value suggests that our model achieves a better performance in binary classification tasks and
 701 vice versa.

$$AUC = \int_0^1 TPR(FPR) d(FPR) \quad (9)$$

702 *RMSE* (Root Mean Square Error) is used to evaluate the efficiency of our model in regression tasks.
 703 It measures the average magnitude of the deviations between predicted values (\hat{y}_i) and actual values
 704 (y_i). A smaller *RMSE* model indicates a better fit of the model to the data.

$$RMSE = \sqrt{\frac{1}{n} \sum_{i=1}^n (y_i - \hat{y}_i)^2} \quad (10)$$

705 Low-Order Statistics.

706 *Column-wise Density Estimation* between numerical features is achieved with the Kolmogorov-
 707 Smirnov Test (KST). The Kolmogorov-Smirnov statistic is used to evaluate how much two underlying
 708 one-dimensional probability distributions differ, and is characterized by the below equation:

$$KST = \sup_x |F_1(x) - F_2(x)|, \quad (11)$$

709 where $F_n(x)$, the empirical distribution function of sample n is calculated by

$$F_n(x) = \frac{1}{n} \sum_{i=1}^n \mathbf{1}_{(-\infty, x]}(X_i) \quad (12)$$

710
 711 *Column-wise Density Estimation* between two categorical features is determined by calculating
 712 the Total Variation Distance (TVD). This statistic captures the largest possible difference in the
 713 probability of any event under two different probability distributions. It is expressed as

$$TVD = \frac{1}{2} \sum_{x \in X} |P_1(x) - P_2(x)|, \quad (13)$$

714 where $P_1(x)$ and $P_2(x)$ are the probabilities (PMF) assigned to data point x by the two sample
 715 distributions respectively.
 716

717 *Pair-wise Column Correlation* between two numerical features is computed using the Pearson
 718 Correlation Coefficient (PCC). It assigns a numerical value to represent the linear relationship

719 between two columns, ranging from -1 (perfect negative linear correlation) to +1 (perfect positive
720 linear correlation), with 0 indicating no linear correlation. It is computed as:

$$\rho(x, y) = \frac{\text{cov}(x, y)}{\sigma_x \sigma_y}, \quad (14)$$

721 To compare the Pearson Coefficients of our real and synthetic datasets, we quantify the dissimilarity
722 in pair-wise column correlation between two samples

$$\text{Pearson Score} = \frac{1}{2} \mathbb{E}_{x, y} |\rho^1(x, y) - \rho^2(x, y)| \quad (15)$$

723 *Pair-wise Column Correlation* between two categorical features in a sample is characterized by
724 a Contingency Table. This table is constructed by tabulating the frequencies at which specific
725 combinations of the levels of two categorical variables work and recording them in a matrix format.

726 To Quantify the dissimilarity of contingency matrices between two different samples, we use the
727 notion of the Contingency Score.

$$\text{Contingency Score} = \frac{1}{2} \sum_{\alpha \in A} \sum_{\beta \in B} |P_{1,(\alpha, \beta)} - P_{2,(\alpha, \beta)}|, \quad (16)$$

728 where α and β describe possible categorical values that can be taken in features A and B . $P_{1,(\alpha, \beta)}$
729 and $P_{2,(\alpha, \beta)}$ refer to the contingency tables representing the features α and β in our two samples,
730 which in this case corresponds to the real and synthetic datasets.

731 In order to obtain the column-wise density estimation and pair-wise correlation between a categorical
732 and a numerical feature, we bin the numerical data into discrete categories before applying TVD and
733 Contingency score respectively to obtain our low-order statistics.

734 We utilize the implementation of these experiments as provided by the SDMetrics library¹.

735 High-Order Statistics

736 We utilize the implementations of High-Order Statistics as provided by the synthcity² library.

737
738 α -precision measures the overall fidelity of the generated data and is an extension of the
739 classical machine learning quality metric of "precision". This formulation is based on the assumption
740 that α fraction of our real samples are characteristic of the original data distribution and the rest are
741 outliers. α -precision therefore quantifies the percentage of generated synthetic samples that match α
742 fraction of real samples (Alaa et al., 2022).

743
744 β -recall characterizes the diversity of our synthetic data and is similarly based on the qual-
745 ity metric of "recall". β -recall shares a similar assumption as α -precision, except that we now assume
746 that β fraction of our synthetic samples are characteristic of the distribution. Therefore, this measure
747 obtains the fraction of the original data distribution that is represented by the β fraction of our
748 generated samples (Alaa et al., 2022).

749 Detection Metric: Classifier Two-Sample Test (C2ST)

750 The Classifier Two-Sample Test, a detection metric, assesses the ability to distinguish real data from
751 synthetic data. This is done through a machine learning model that attempts to label whether a data
752 point is synthetic or real. The score ranges from 0 to 1 where a score closer to 1 is superior, as
753 it indicates that the machine learning model cannot concretely identify whether the data point in
754 question is real or generated. We select logistic regression as our machine learning model in this case,
755 using the implementation provided by SDMetric (SDMetrics, 2024).

756 Privacy Metric: Distance to Closest Record (DCR)

757 The Distance to Closest Record metric quantifies the distance between each generated sample to our
758 training set. The score is calculated as the proportion of synthetic data points that have a closer match

¹<https://github.com/sdv-dev/SDMetrics>

²<https://github.com/vanderschaarlab/synthcity>

759 to the real data set compared to the holdout set. A score close to 50% is ideal, as it indicates that our
760 generated sample represents the underlying distribution of our training samples without revealing
761 specific points present in the dataset.

762 **D Further Experimental Results**

763 We run all experiments outlined in this section on at least 4 main models: TabUnite-i2bFlow,
 764 TabUnite-dicFlow, TabSYN(Zhang et al., 2023), and TabDDPM(Kotelnikov et al., 2023) due to their
 765 competitive performance on our MLE experiments as seen in Table 1 as well as prior literature (Zhang
 766 et al., 2023). Unless otherwise stated, we use experimental results collected by TabSYN’s author for
 767 all other model benchmarks. The metrics and error bars shown in the tables in this section are derived
 768 from the mean and standard deviation of experiments performed on 20 randomly sampled sets of
 769 synthetic data.

770 **D.1 Training and Sampling Time**

771 We showcase the training and sampling durations for TabUnite and other competitive diffusion-based
 772 baseline models obtained from our experiments in this section. Experiments for all datasets outlined
 773 in table Table 9 are performed in the computing environment described in section Appendix C. For
 774 the two TabUnite methods (i2bFlow and dicFlow) and the flow-matching-based baseline TabFlow,
 775 we use the hyperparameters as specified in Table 3. For all non-TabUnite methods, we follow the
 776 recommended parameters set forth by their respective authors, see (Kim et al., 2022), (Lee et al.,
 2023), (Kotelnikov et al., 2023), and (Zhang et al., 2023).

Table 9: Training and Sampling Times of TabUnite and baselines on the Beijing Dataset. The hyperparameters used to run these experiments are included in Table 3.

Model	Training Time (s)	Training Steps	Training Time/step (s)	Sampling Time (s)
STaSy	8029.92	10,000	0.803	17.39
CoDi	30342.05	20,000	1.517	11.15
TabDDPM	4188.56	100,000	0.042	73.82
TabSYN	3671.48	4,000+625	0.509	5.97
TabFlow	6772.25	100,000	0.068	3.87
TabUnite-i2bFlow	5182.89	100,000	0.052	3.80
TabUnite-dicFlow	4380.02	100,000	0.044	3.40

777 Note that for TabSYN, the VAE is trained for 4000 steps, taking 3352.70 seconds to complete. Early
 778 stopping when training the EDM model is reached at 625/10001 epochs, finishing in an additional
 779 318.78 seconds. The training times presented in the figure are the sum of the times required to
 780 complete training on both the VAE and diffusion models.
 781
 782

783 **D.2 Low-order statistics: Column-wise density estimation and Pair-wise column correlation**

784 The results for our Low-Order metrics tests can be found in Table 10 and Table 11.

Table 10: Error rate (%) of column-wise density estimation. Values bolded in red and blue are the best and second best-performing models respectively for each dataset.

Method	Adult	Default	Shoppers	Magic	Beijing	News	Overall Rank
SMOTE	1.60±0.23	1.48±0.15	2.68±0.19	0.91±0.05	1.85±0.21	5.31±0.46	N/A
CTGAN	16.84±0.03	16.83±0.04	21.15±0.10	9.81±0.08	21.39±0.05	16.09±0.02	8
TVAE	14.22±0.08	10.17±0.05	24.51±0.06	8.25±0.06	19.16±0.06	16.62±0.03	7
GOGGLE	16.97	17.02	22.33	1.90	16.93	25.32	6
GReaT	12.12±0.04	19.94±0.06	14.51±0.12	16.16±0.09	8.25±0.12	OOM	9
STaSy	11.29±0.06	5.77±0.06	9.37±0.09	6.29±0.13	6.71±0.03	6.89±0.03	4
CoDi	21.38±0.06	15.77±0.07	31.84±0.05	11.56±0.26	16.94±0.02	32.27±0.04	10
TabDDPM	1.37±0.05	2.06±0.06	4.49±0.09	2.64±0.19	49.25±0.13	75.11±0.03	4
TabSYN	3.96±0.08	2.90±0.04	2.56±0.07	2.65±0.12	2.24±0.04	5.74±0.05	3
TabUnite-i2bFlow	1.19±0.05	2.17±0.09	3.19±0.10	2.54±0.20	2.49±0.04	2.81±0.03	1
TabUnite-dicFlow	1.64±0.06	2.70±0.07	3.14±0.07	3.09±0.19	2.10±0.06	3.31±0.04	2

Table 11: Error rate (%) of pair-wise column correlation score. Values bolded in **red** and **blue** are the best and second best-performing models respectively for each dataset.

Method	Adult	Default	Shoppers	Magic	Beijing	News	Overall Rank
SMOTE	3.28±0.29	8.41±0.38	3.56±0.22	3.16±0.41	2.39±0.35	5.38±0.76	N/A
CTGAN	20.23±1.20	26.95±0.93	13.08±0.16	7.00±0.19	22.95±0.08	5.37±0.05	7
TVAE	14.15±0.88	19.50±0.95	18.67±0.38	5.82±0.49	18.01±0.08	6.17±0.09	6
GOGGLE	45.29	21.94	23.90	9.47	45.94	23.19	9
GReaT	17.59±0.22	70.02±0.12	45.16±0.18	10.23±0.40	59.60±0.55	OOM	10
STaSy	14.51±0.25	5.96±0.26	8.49±0.15	6.61±0.53	8.00±0.10	3.07±0.04	4
CoDi	22.49±0.08	68.41±0.05	17.78±0.11	6.53±0.25	7.07±0.15	11.10±0.01	7
TabDDPM	2.67±0.05	13.56±0.16	11.89±0.09	2.27±0.09	50.76±0.08	15.65±0.23	5
TabSYN	6.64±0.15	12.44±1.02	6.45±0.08	3.19±0.12	5.80±0.13	4.16±0.03	3
TabUnite-i2bFlow	2.95±0.37	11.69±1.19	6.04±0.55	3.18±0.46	5.71±0.10	2.48±0.03	1
TabUnite-dicFlow	3.63±0.35	11.46±1.78	7.28±0.33	3.28±0.45	5.65±0.13	2.74±0.09	2

785 D.3 High-order metrics: α -precision and β -recall

786 The results for our High-Order metrics tests can be found in Table 12 and Table 13.

787 Note that similar to the results obtained in TabSYN’s paper, TabDDPM also collapses on the News
788 dataset in our experiments.

Table 12: Comparison of α -Precision scores. Higher values indicate superior results. Values bolded in **red** and **blue** are the best and second best-performing models respectively for each dataset.

Methods	Adult	Default	Shoppers	Magic	Beijing	News	Overall Rank
CTGAN	77.74±0.15	62.08±0.08	76.97±0.39	86.90±0.22	96.27±0.14	96.96±0.17	8
TVAE	98.17±0.17	85.57±0.34	58.19±0.26	86.19±0.48	97.20±0.10	86.41±0.17	7
GOGGLE	50.68	68.89	86.95	90.88	88.81	86.41	10
GReaT	55.79±0.03	85.90±0.17	78.88±0.13	85.46±0.54	98.32±0.22	-	8
STaSy	82.87±0.26	90.48±0.11	89.65±0.25	86.56±0.19	89.16±0.12	94.76±0.33	5
CoDi	77.58±0.45	82.38±0.15	94.95±0.35	85.01±0.36	98.13±0.38	87.15±0.12	6
TabDDPM	94.79±0.27	98.27±0.34	98.33±0.40	93.35±0.53	0.01±0.73	0.00±0.00	4
TabSYN	98.51±0.31	98.73±0.20	98.80±0.36	98.01±0.30	97.30±0.30	97.98±0.08	3
TabUnite-i2bFlow	99.42±0.13	97.08±0.33	98.78±0.47	99.10±0.20	97.60±0.27	98.77±0.39	1
TabUnite-dicFlow	99.27±0.2	96.16±0.34	97.34±0.55	99.27±0.19	98.90±0.22	98.47±0.29	2

Table 13: Comparison of β -Recall scores. Higher values indicate superior results. Values bolded in **red** and **blue** are the best and second best-performing models respectively for each dataset.

Methods	Adult	Default	Shoppers	Magic	Beijing	News	Overall Rank
CTGAN	30.80±0.20	18.22±0.17	31.80±0.350	11.75±0.20	34.80±0.10	24.97±0.29	9
TVAE	38.87±0.31	23.13±0.11	19.78±0.10	32.44±0.35	28.45±0.08	29.66±0.21	8
GOGGLE	8.80	14.38	9.79	9.88	19.87	2.03	10
GReaT	49.12±0.18	42.04±0.19	44.90±0.17	34.91±0.28	43.34±0.31	-	6
STaSy	29.21±0.34	39.31±0.39	37.24±0.45	53.97±0.57	54.79±0.18	39.42±0.32	4
CoDi	9.20±0.15	19.94±0.22	20.82±0.23	50.56±0.31	52.19±0.12	34.40±0.31	7
TabDDPM	50.74±0.37	46.90±0.35	53.32±0.52	46.26±0.35	0.02±0.68	0.00±0.00	5
TabSYN	45.13±0.23	44.30±0.29	48.68±0.57	45.28±0.40	55.50±0.21	35.70±0.18	3
TabUnite-i2bFlow	48.49±0.17	47.43±0.33	54.47±0.57	67.60±0.28	60.34±0.20	50.89±0.27	2
TabUnite-dicFlow	51.34±0.25	50.75±0.34	52.24±0.59	66.93±0.19	60.66±0.21	50.07±0.29	1

789 **D.4 Detection metric: Classifier Two-Sample Test (C2ST)**

790 The results for our C2ST tests can be found in Table 14. We are generally competitive with TabSYN
 791 and TabDDPM.

Table 14: Comparison of C2ST scores. Higher values indicate superior results. Values bolded in **red** and **blue** are the best and second best-performing models respectively for each dataset.

Methods	Adult	Default	Shoppers	Magic	Beijing	News	Overall Rank
CTGAN	0.5949	0.4875	0.7488	0.6728	0.7531	0.6947	7
TVAE	0.6315	0.6547	0.2962	0.7706	0.8659	0.4076	5
GOGLE	0.1114	0.5163	0.1418	0.9526	0.4779	0.0745	8
GReaT	0.5376	0.4710	0.4285	0.4326	0.6893	-	9
STaSy	0.4054	0.6814	0.5482	0.6939	0.7922	0.5287	6
CoDi	0.2077	0.4595	0.2784	0.7206	0.7177	0.0201	10
TabDDPM	0.1263	0.9844	0.8545	0.9951	0.0380	0.0000	4
TabSYN	0.9235	0.9664	0.9516	0.9526	0.8937	0.7934	1
TabUnite-i2bFlow	0.7180	0.9407	0.8538	0.9304	0.9304	0.9005	3
TabUnite-dicFlow	0.9004	0.9275	0.9176	0.9514	0.9477	0.8784	2

792 **D.5 Privacy metric: Distance to Closest Record**

793 The results for our DCR tests can be found in Table 15. As observed, we remain competitive but do
 794 not outperform TabSYN as the best method under this metric. This aligns with our hypothesis where
 TabSYN leverages a latent space thus, resulting in a lossy compression, improving their DCR scores.

Table 15: Comparison of DCR. Results closer to 50% indicate better performance on the test. Values bolded in **red** and **blue** are the best and second best-performing models respectively for each dataset.

Methods	Adult	Default	Shoppers	Magic	Beijing	News	Overall Rank
TabDDPM	81.92±0.13	64.05±0.18	91.49±0.07	63.51±0.47	82.44±0.09	59.09±0.16	0.00
TabSYN	51.67±0.35	50.87±0.17	52.05±0.88	52.10±0.39	51.55±0.38	50.72±0.25	0.0
TabUnite-i2bFlow	53.87±0.27	52.96±0.44	59.66±0.54	83.71±0.28	54.33±0.65	55.81±0.11	0.00
TabUnite-dicFlow	65.35±0.04	57.79±0.26	72.16±0.65	82.90±0.46	60.97±0.25	55.76±0.51	0.00

795

796 **NeurIPS Paper Checklist**

797 **1. Claims**

798 Question: Do the main claims made in the abstract and introduction accurately reflect the
799 paper’s contributions and scope?

800 Answer: [Yes]

801 Justification: We elaborate the model architecture as well as encoding methods introduced
802 in the abstract in depth in Section 3, with visual diagrams presented in Figure 1 and
803 Figure 2. The claims on our model’s performance are backed by Table 1, Table 7 where we
804 highlighted the highest-performing models for each dataset, as well as various other results
805 in the appendix.

806 Guidelines:

- 807 • The answer NA means that the abstract and introduction do not include the claims
808 made in the paper.
- 809 • The abstract and/or introduction should clearly state the claims made, including the
810 contributions made in the paper and important assumptions and limitations. A No or
811 NA answer to this question will not be perceived well by the reviewers.
- 812 • The claims made should match theoretical and experimental results, and reflect how
813 much the results can be expected to generalize to other settings.
- 814 • It is fine to include aspirational goals as motivation as long as it is clear that these goals
815 are not attained by the paper.

816 **2. Limitations**

817 Question: Does the paper discuss the limitations of the work performed by the authors?

818 Answer: [Yes]

819 Justification: A limitation of our methodology is that we have not extensively explored a
820 continuous embedding scheme where we perform the reverse and unify the generative space
821 into a categorical one. Inspired by (Ansari et al., 2024), we conduct initial explorations of
822 time series tokenization to embed continuous features yet, our results are still inconclusive
823 and left to future work.

824 Guidelines:

- 825 • The answer NA means that the paper has no limitation while the answer No means that
826 the paper has limitations, but those are not discussed in the paper.
- 827 • The authors are encouraged to create a separate "Limitations" section in their paper.
- 828 • The paper should point out any strong assumptions and how robust the results are to
829 violations of these assumptions (e.g., independence assumptions, noiseless settings,
830 model well-specification, asymptotic approximations only holding locally). The authors
831 should reflect on how these assumptions might be violated in practice and what the
832 implications would be.
- 833 • The authors should reflect on the scope of the claims made, e.g., if the approach was
834 only tested on a few datasets or with a few runs. In general, empirical results often
835 depend on implicit assumptions, which should be articulated.
- 836 • The authors should reflect on the factors that influence the performance of the approach.
837 For example, a facial recognition algorithm may perform poorly when image resolution
838 is low or images are taken in low lighting. Or a speech-to-text system might not be
839 used reliably to provide closed captions for online lectures because it fails to handle
840 technical jargon.
- 841 • The authors should discuss the computational efficiency of the proposed algorithms
842 and how they scale with dataset size.
- 843 • If applicable, the authors should discuss possible limitations of their approach to
844 address problems of privacy and fairness.
- 845 • While the authors might fear that complete honesty about limitations might be used by
846 reviewers as grounds for rejection, a worse outcome might be that reviewers discover
847 limitations that aren’t acknowledged in the paper. The authors should use their best

848 judgment and recognize that individual actions in favor of transparency play an impor-
849 tant role in developing norms that preserve the integrity of the community. Reviewers
850 will be specifically instructed to not penalize honesty concerning limitations.

851 3. Theory Assumptions and Proofs

852 Question: For each theoretical result, does the paper provide the full set of assumptions and
853 a complete (and correct) proof?

854 Answer: [NA]

855 Justification: We do not include theoretical results in our paper.

856 Guidelines:

- 857 • The answer NA means that the paper does not include theoretical results.
- 858 • All the theorems, formulas, and proofs in the paper should be numbered and cross-
859 referenced.
- 860 • All assumptions should be clearly stated or referenced in the statement of any theorems.
- 861 • The proofs can either appear in the main paper or the supplemental material, but if
862 they appear in the supplemental material, the authors are encouraged to provide a short
863 proof sketch to provide intuition.
- 864 • Inversely, any informal proof provided in the core of the paper should be complemented
865 by formal proofs provided in appendix or supplemental material.
- 866 • Theorems and Lemmas that the proof relies upon should be properly referenced.

867 4. Experimental Result Reproducibility

868 Question: Does the paper fully disclose all the information needed to reproduce the main ex-
869 perimental results of the paper to the extent that it affects the main claims and/or conclusions
870 of the paper (regardless of whether the code and data are provided or not)?

871 Answer: [Yes]

872 Justification: Detailed experimental setup, methodologies, and chosen parameters are shown
873 in Appendix. We evaluate our models on a variety of metrics and tests. **A**, **B**, and **C**.

874 Guidelines:

- 875 • The answer NA means that the paper does not include experiments.
- 876 • If the paper includes experiments, a No answer to this question will not be perceived
877 well by the reviewers: Making the paper reproducible is important, regardless of
878 whether the code and data are provided or not.
- 879 • If the contribution is a dataset and/or model, the authors should describe the steps taken
880 to make their results reproducible or verifiable.
- 881 • Depending on the contribution, reproducibility can be accomplished in various ways.
882 For example, if the contribution is a novel architecture, describing the architecture fully
883 might suffice, or if the contribution is a specific model and empirical evaluation, it may
884 be necessary to either make it possible for others to replicate the model with the same
885 dataset, or provide access to the model. In general, releasing code and data is often
886 one good way to accomplish this, but reproducibility can also be provided via detailed
887 instructions for how to replicate the results, access to a hosted model (e.g., in the case
888 of a large language model), releasing of a model checkpoint, or other means that are
889 appropriate to the research performed.
- 890 • While NeurIPS does not require releasing code, the conference does require all submis-
891 sions to provide some reasonable avenue for reproducibility, which may depend on the
892 nature of the contribution. For example
 - 893 (a) If the contribution is primarily a new algorithm, the paper should make it clear how
894 to reproduce that algorithm.
 - 895 (b) If the contribution is primarily a new model architecture, the paper should describe
896 the architecture clearly and fully.
 - 897 (c) If the contribution is a new model (e.g., a large language model), then there should
898 either be a way to access this model for reproducing the results or a way to reproduce
899 the model (e.g., with an open-source dataset or instructions for how to construct
900 the dataset).

901 (d) We recognize that reproducibility may be tricky in some cases, in which case
902 authors are welcome to describe the particular way they provide for reproducibility.
903 In the case of closed-source models, it may be that access to the model is limited in
904 some way (e.g., to registered users), but it should be possible for other researchers
905 to have some path to reproducing or verifying the results.

906 5. Open access to data and code

907 Question: Does the paper provide open access to the data and code, with sufficient instruc-
908 tions to faithfully reproduce the main experimental results, as described in supplemental
909 material?

910 Answer: [Yes]

911 Justification: The code is anonymised and zipped along with our submission.

912 Guidelines:

- 913 • The answer NA means that paper does not include experiments requiring code.
- 914 • Please see the NeurIPS code and data submission guidelines ([https://nips.cc/
915 public/guides/CodeSubmissionPolicy](https://nips.cc/public/guides/CodeSubmissionPolicy)) for more details.
- 916 • While we encourage the release of code and data, we understand that this might not be
917 possible, so “No” is an acceptable answer. Papers cannot be rejected simply for not
918 including code, unless this is central to the contribution (e.g., for a new open-source
919 benchmark).
- 920 • The instructions should contain the exact command and environment needed to run to
921 reproduce the results. See the NeurIPS code and data submission guidelines ([https:
922 //nips.cc/public/guides/CodeSubmissionPolicy](https://nips.cc/public/guides/CodeSubmissionPolicy)) for more details.
- 923 • The authors should provide instructions on data access and preparation, including how
924 to access the raw data, preprocessed data, intermediate data, and generated data, etc.
- 925 • The authors should provide scripts to reproduce all experimental results for the new
926 proposed method and baselines. If only a subset of experiments are reproducible, they
927 should state which ones are omitted from the script and why.
- 928 • At submission time, to preserve anonymity, the authors should release anonymized
929 versions (if applicable).
- 930 • Providing as much information as possible in supplemental material (appended to the
931 paper) is recommended, but including URLs to data and code is permitted.

932 6. Experimental Setting/Details

933 Question: Does the paper specify all the training and test details (e.g., data splits, hyper-
934 parameters, how they were chosen, type of optimizer, etc.) necessary to understand the
935 results?

936 Answer: [Yes]

937 Justification: Data splits can be found in Appendix C.1. We provide a detailed list of our
938 hyperparameters in Table 3. We explicitly state in the section that we utilize the same
939 parameters as two prior models to ensure that experimental results are commensurable.

940 Guidelines:

- 941 • The answer NA means that the paper does not include experiments.
- 942 • The experimental setting should be presented in the core of the paper to a level of detail
943 that is necessary to appreciate the results and make sense of them.
- 944 • The full details can be provided either with the code, in appendix, or as supplemental
945 material.

946 7. Experiment Statistical Significance

947 Question: Does the paper report error bars suitably and correctly defined or other appropriate
948 information about the statistical significance of the experiments?

949 Answer: [Yes]

950 Justification: We provide standard deviation error bars for our experimental results when
951 permissible. Specifically, this is shown in our tables.

952 Guidelines:

- 953 • The answer NA means that the paper does not include experiments.
- 954 • The authors should answer "Yes" if the results are accompanied by error bars, confi-
- 955 dence intervals, or statistical significance tests, at least for the experiments that support
- 956 the main claims of the paper.
- 957 • The factors of variability that the error bars are capturing should be clearly stated (for
- 958 example, train/test split, initialization, random drawing of some parameter, or overall
- 959 run with given experimental conditions).
- 960 • The method for calculating the error bars should be explained (closed form formula,
- 961 call to a library function, bootstrap, etc.)
- 962 • The assumptions made should be given (e.g., Normally distributed errors).
- 963 • It should be clear whether the error bar is the standard deviation or the standard error
- 964 of the mean.
- 965 • It is OK to report 1-sigma error bars, but one should state it. The authors should
- 966 preferably report a 2-sigma error bar than state that they have a 96% CI, if the hypothesis
- 967 of Normality of errors is not verified.
- 968 • For asymmetric distributions, the authors should be careful not to show in tables or
- 969 figures symmetric error bars that would yield results that are out of range (e.g. negative
- 970 error rates).
- 971 • If error bars are reported in tables or plots, The authors should explain in the text how
- 972 they were calculated and reference the corresponding figures or tables in the text.

973 8. Experiments Compute Resources

974 Question: For each experiment, does the paper provide sufficient information on the com-
 975 puter resources (type of compute workers, memory, time of execution) needed to reproduce
 976 the experiments?

977 Answer: [Yes]

978 Justification: We introduce in Appendix C the computer resources used in our experiments.
 979 The compute required for experimental runs are detailed in Table 9.

980 Guidelines:

- 981 • The answer NA means that the paper does not include experiments.
- 982 • The paper should indicate the type of compute workers CPU or GPU, internal cluster,
- 983 or cloud provider, including relevant memory and storage.
- 984 • The paper should provide the amount of compute required for each of the individual
- 985 experimental runs as well as estimate the total compute.
- 986 • The paper should disclose whether the full research project required more compute
- 987 than the experiments reported in the paper (e.g., preliminary or failed experiments that
- 988 didn't make it into the paper).

989 9. Code Of Ethics

990 Question: Does the research conducted in the paper conform, in every respect, with the
 991 NeurIPS Code of Ethics <https://neurips.cc/public/EthicsGuidelines?>

992 Answer: [Yes]

993 Justification: With have adhered to the NeurIPS Code of Ethics when conducting our
 994 research on this paper.

995 Guidelines:

- 996 • The answer NA means that the authors have not reviewed the NeurIPS Code of Ethics.
- 997 • If the authors answer No, they should explain the special circumstances that require a
- 998 deviation from the Code of Ethics.
- 999 • The authors should make sure to preserve anonymity (e.g., if there is a special consid-
- 1000 eration due to laws or regulations in their jurisdiction).

1001 10. Broader Impacts

1002 Question: Does the paper discuss both potential positive societal impacts and negative
 1003 societal impacts of the work performed?

1004 Answer: [NA]

1005 Justification: Our work on tabular data generation does not include potential malicious or
1006 unintended uses or impact specific groups. It does not violate privacy and security concerns
1007 either.

1008 Guidelines:

- 1009 • The answer NA means that there is no societal impact of the work performed.
- 1010 • If the authors answer NA or No, they should explain why their work has no societal
1011 impact or why the paper does not address societal impact.
- 1012 • Examples of negative societal impacts include potential malicious or unintended uses
1013 (e.g., disinformation, generating fake profiles, surveillance), fairness considerations
1014 (e.g., deployment of technologies that could make decisions that unfairly impact specific
1015 groups), privacy considerations, and security considerations.
- 1016 • The conference expects that many papers will be foundational research and not tied
1017 to particular applications, let alone deployments. However, if there is a direct path to
1018 any negative applications, the authors should point it out. For example, it is legitimate
1019 to point out that an improvement in the quality of generative models could be used to
1020 generate deepfakes for disinformation. On the other hand, it is not needed to point out
1021 that a generic algorithm for optimizing neural networks could enable people to train
1022 models that generate Deepfakes faster.
- 1023 • The authors should consider possible harms that could arise when the technology is
1024 being used as intended and functioning correctly, harms that could arise when the
1025 technology is being used as intended but gives incorrect results, and harms following
1026 from (intentional or unintentional) misuse of the technology.
- 1027 • If there are negative societal impacts, the authors could also discuss possible mitigation
1028 strategies (e.g., gated release of models, providing defenses in addition to attacks,
1029 mechanisms for monitoring misuse, mechanisms to monitor how a system learns from
1030 feedback over time, improving the efficiency and accessibility of ML).

1031 11. Safeguards

1032 Question: Does the paper describe safeguards that have been put in place for responsible
1033 release of data or models that have a high risk for misuse (e.g., pretrained language models,
1034 image generators, or scraped datasets)?

1035 Answer: [NA]

1036 Justification: One of our main contributions, a large mixed-type tabular dataset, is curated
1037 from augmenting a public-domain dataset based on anonymised US census data in 1990
1038 (Dua & Graff, 2017), which poses a very low risk for potential misuse.

1039 Guidelines:

- 1040 • The answer NA means that the paper poses no such risks.
- 1041 • Released models that have a high risk for misuse or dual-use should be released with
1042 necessary safeguards to allow for controlled use of the model, for example by requiring
1043 that users adhere to usage guidelines or restrictions to access the model or implementing
1044 safety filters.
- 1045 • Datasets that have been scraped from the Internet could pose safety risks. The authors
1046 should describe how they avoided releasing unsafe images.
- 1047 • We recognize that providing effective safeguards is challenging, and many papers do
1048 not require this, but we encourage authors to take this into account and make a best
1049 faith effort.

1050 12. Licenses for existing assets

1051 Question: Are the creators or original owners of assets (e.g., code, data, models), used in
1052 the paper, properly credited and are the license and terms of use explicitly mentioned and
1053 properly respected?

1054 Answer: [Yes]

1055 Justification: We properly acknowledge and cite all assets and resources used in the paper.
1056 The license of the datasets is also explicitly mentioned as the CC-BY 4.0 license in our
1057 Appendix.

1058
1059
1060
1061
1062
1063
1064
1065
1066
1067
1068
1069
1070
1071
1072
1073
1074
1075
1076
1077
1078
1079
1080
1081
1082
1083
1084
1085
1086
1087
1088
1089
1090
1091
1092
1093
1094
1095
1096
1097
1098
1099
1100
1101
1102
1103
1104
1105
1106
1107
1108
1109
1110

Guidelines:

- The answer NA means that the paper does not use existing assets.
- The authors should cite the original paper that produced the code package or dataset.
- The authors should state which version of the asset is used and, if possible, include a URL.
- The name of the license (e.g., CC-BY 4.0) should be included for each asset.
- For scraped data from a particular source (e.g., website), the copyright and terms of service of that source should be provided.
- If assets are released, the license, copyright information, and terms of use in the package should be provided. For popular datasets, paperswithcode.com/datasets has curated licenses for some datasets. Their licensing guide can help determine the license of a dataset.
- For existing datasets that are re-packaged, both the original license and the license of the derived asset (if it has changed) should be provided.
- If this information is not available online, the authors are encouraged to reach out to the asset's creators.

13. New Assets

Question: Are new assets introduced in the paper well documented and is the documentation provided alongside the assets?

Answer: [Yes]

Justification: We introduce a new dataset, Census Synthetic, with proper documentation on how the dataset is curated in the Appendix. License is also based on the existing Census dataset where it is CC-BY 4.0.

Guidelines:

- The answer NA means that the paper does not release new assets.
- Researchers should communicate the details of the dataset/code/model as part of their submissions via structured templates. This includes details about training, license, limitations, etc.
- The paper should discuss whether and how consent was obtained from people whose asset is used.
- At submission time, remember to anonymize your assets (if applicable). You can either create an anonymized URL or include an anonymized zip file.

14. Crowdsourcing and Research with Human Subjects

Question: For crowdsourcing experiments and research with human subjects, does the paper include the full text of instructions given to participants and screenshots, if applicable, as well as details about compensation (if any)?

Answer: [NA]

Justification: The paper does not involve crowdsourcing nor research with human subjects

Guidelines:

- The answer NA means that the paper does not involve crowdsourcing nor research with human subjects.
- Including this information in the supplemental material is fine, but if the main contribution of the paper involves human subjects, then as much detail as possible should be included in the main paper.
- According to the NeurIPS Code of Ethics, workers involved in data collection, curation, or other labor should be paid at least the minimum wage in the country of the data collector.

15. Institutional Review Board (IRB) Approvals or Equivalent for Research with Human Subjects

Question: Does the paper describe potential risks incurred by study participants, whether such risks were disclosed to the subjects, and whether Institutional Review Board (IRB) approvals (or an equivalent approval/review based on the requirements of your country or institution) were obtained?

1111
1112
1113
1114
1115
1116
1117
1118
1119
1120
1121
1122
1123

Answer: [NA]

Justification: The paper does not involve crowdsourcing nor research with human subjects.

Guidelines:

- The answer NA means that the paper does not involve crowdsourcing nor research with human subjects.
- Depending on the country in which research is conducted, IRB approval (or equivalent) may be required for any human subjects research. If you obtained IRB approval, you should clearly state this in the paper.
- We recognize that the procedures for this may vary significantly between institutions and locations, and we expect authors to adhere to the NeurIPS Code of Ethics and the guidelines for their institution.
- For initial submissions, do not include any information that would break anonymity (if applicable), such as the institution conducting the review.